

CARDIAC EFFECTS OF RECURRING AUTONOMIC DYSREFLEXIA

by

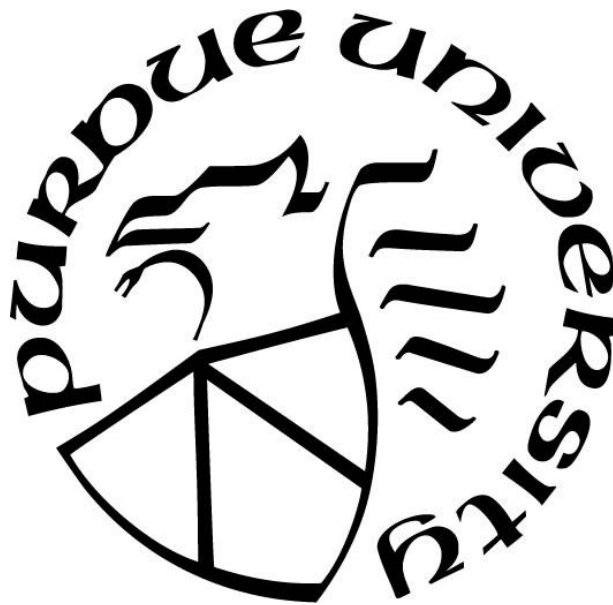
Zada B. Anderson

A Thesis

Submitted to the Faculty of Purdue University

In Partial Fulfillment of the Requirements for the degree of

Master of Science in Biomedical Engineering



Weldon School of Biomedical Engineering

West Lafayette, Indiana

August 2023

**THE PURDUE UNIVERSITY GRADUATE SCHOOL
STATEMENT OF COMMITTEE APPROVAL**

Dr. Bradley S. Duerstock, Co-chair

Weldon School of Biomedical Engineering

School of Industrial Engineering

Dr. Thomas H. Everett IV, Co-chair

Krannert Cardiovascular Research Institute

IU School of Medicine

Dr. Riya Shi

Weldon School of Biomedical Engineering

Department of Basic Medical Sciences

Approved by:

Dr. Tamara L. Kinzer-Ursem

Dedicated to my cats.

ACKNOWLEDGMENTS

I would like to thank Dr. Duerstock and Dr. Everett IV for their support throughout the completion of my thesis, meeting with me weekly. I would also like to thank Dr. Shi for acting as a sounding board for animal physiology trend analysis.

I would like to thank Dr. Suresh for introducing me to the project and providing me with the majority of my animal handling training. Thank you to Ana Kirby and Mitch Sanchez for helping with the transition and being available to answer questions from data analysis to lab logistics.

I would also like to extend my gratitude to Molly Dye and Emilie Chadwell for their assistance with rat care, data collection and data analysis.

Dr. Koss and Jennifer Crodian were essential for lab set up and logistics throughout. Thank you to Dr. Darbyshire and Carol Dowell along with all the BME animal care staff for their guidance and training with rat care. Finally, I would like to thank Tammy Siemers and Sandra May for helping me navigate the graduate school logistics.

TABLE OF CONTENTS

LIST OF FIGURES	7
ABSTRACT.....	9
1. INTRODUCTION	10
1.1 Overview.....	10
1.2 Research Problem	11
1.3 Research Questions.....	12
1.4 Contribution	12
1.5 Thesis Structure	12
2. BACKGROUND AND LITERATURE REVIEW	13
2.1 The Autonomic Nervous System.....	13
2.2 Autonomic Dysfunction in Spinal Cord Injury.....	15
2.3 Prevalence of SCI and Autonomic Dysreflexia	17
2.4 Impacts on the Heart and QT Interval.....	18
3. ANIMAL MODEL	20
3.1 Model Selection	20
3.2 Implant Surgery	21
3.3 Acclimation.....	21
3.4 High Thoracic Spinal Cord Injury Surgery.....	23
3.5 Post SCI Care.....	23
3.6 Sensors	24
3.7 Induction of AD	24
3.8 Signal Processing.....	26
4. GENERAL BEHAVIORS.....	30
4.1 Autonomic Dysreflexia vs. Baseline.....	30
4.2 SKNA Bursting Activity.....	33
4.3 Overall Insights.....	34
5. LONG TERM CHANGES IN CARDIAC PARAMETERS.....	36
5.1 Blood Pressure Behavior and AD Incidence	36
5.2 ECG Components and Observations	38

5.3	Insights on Long-term Cardiac Effects	46
6.	CONCLUSIONS AND FUTURE DIRECTIONS	48
6.1	Conclusions.....	48
6.2	Limitations and Possible Modifications.....	49
6.3	Future Directions	50
	REFERENCES	51
	PUBLICATIONS.....	59

LIST OF FIGURES

Figure 2.1. Normal autonomic nervous system control of cardiovascular system (La Rovere & Christensen, 2015).	14
Figure 2.2. High level SCI effects on cardiovascular system (Ahuja et al., 2017).....	16
Figure 3.1. Acclimation protocol phases.	22
Figure 3.2. (a) Lead 1 placement of external electrodes and (b) External electrodes, alligator clamps, and snuggle.....	24
Figure 3.3. Experimental setup with external electrodes, alligator clamps, snuggle, restraint tube, blackout box, and foley catheter.	25
Figure 3.4. 3D printed syringe holder for catheter inflation.....	25
Figure 3.5. Burst detection example. Bursts are represented by the red sections.....	26
Figure 3.6. Peak detection results.	27
Figure 3.7. Tangent method of finding the T-wave end point for QT calculations.....	28
Figure 3.8. Removal of calculated values influenced by 1-volt shock. The vertical red lines which surround the vertical black line represent the start and end points of data removal due to the 1-volt shock.....	29
Figure 4.1. Comparison of QTc and STVQTc for baseline, AD, and non-AD (NAD) conditions (*p < 0.05).....	30
Figure 4.2. Baseline vs. AD comparisons (N = 10 rats) (*p < 0.05). Blood pressure, P-wave height, and QRS width were significantly different between AD and Baseline.....	32
Figure 4.3. SKNA bursting activity with QTc behavior.....	33
Figure 4.4. Comparison of QTc during SKNA bursting and non-bursting (N = 10 rats) (*p < 0.05).	33
Figure 4.5. Comparison of STVQTc during SKNA bursting and non-bursting (N = 10 rats) (*p < 0.05).	34
Figure 5.1. AD incidence across the 21 days post injury (N = 10).....	36
Figure 5.2. Systolic blood pressure peak value above threshold during AD events (*p < 0.05)..	37
Figure 5.3. Peak above threshold count during AD events.....	38
Figure 5.4. Change in QTc throughout experiment (*p < 0.05).	39
Figure 5.5. Change in STVQTc throughout experiment (*p < 0.05).....	40
Figure 5.6. Example of a PVC.....	41
Figure 5.7. Change in systolic blood pressure post SCI (*p < 0.05).	42

Figure 5.8. Change in heart rate post SCI (*p < 0.05).....	43
Figure 5.9. Change in R-R interval post SCI (*p < 0.05).....	44
Figure 5.10. Change in P-wave height post SCI (*p < 0.05).....	45
Figure 5.11. Change in QRS width post SCI (*p < 0.05).....	46

ABSTRACT

Persons with a spinal cord injury (SCI) above the sixth thoracic vertebrae commonly experience autonomic dysreflexia (AD), 90 percent of individuals with this level of injury are susceptible to AD which is associated with an increase in sympathetic nerve activity. Left untreated AD causes a paroxysmal rise in blood pressure that may result in seizures, heart attack, or even death. This project investigates how AD affects QT interval, RR interval, P wave height, heart rate, and QRS width both during an event and long term to help identify potential cardiac risks for individuals with SCI who experience chronic AD. Sympathetic tone has been shown to influence QT interval changes that can be indicative of an increased risk of arrhythmia, which can be exacerbated by recurring episodes of AD.

A rat spinal cord injury model at the T3 level undergoing colorectal distention (CRD) was used to induce AD. Electrophysiological recordings from an implanted ECG sensor and noninvasive skin nerve activity (SKNA) sensor array during normal baseline and three trials of CRD were collected on days 5, 7, 9, 11, 14, 16, 19, and 21 post-SCI. Custom MATLAB algorithms were used to identify the QRS complex and T-peaks from the implant ECG signal. QT interval measurements were taken for 2 minutes of baseline and for 2 minutes after the initiation of each CRD trial. Corrected QT interval (QTc) was calculated using normalized Bazett's formula to account for the impact of heart rate on QT interval.

It was found that the rats' susceptibility and reaction to AD events varied between subacute (5-14 days) and chronic phases of SCI. During the chronic phase the incidence of AD events increased during regular occurrences of CRD as indicated by above-threshold (≥ 15 mmHg) blood pressure spikes. AD events also resulted in increased QT interval short term variability marking an increased risk of arrhythmias. Baseline P-wave height and QTc interval were also increased while QRS complex width decreased resulting in potentially detrimental cardiac effects. This rat model showed that humans who experience recurrent AD during the chronic phase of SCI may be at increased risk for arrhythmia.

1. INTRODUCTION

1.1 Overview

There are approximately 302,000 people with traumatic spinal cord injury (SCI) living in the United States with 18,000 new cases every year (National Spinal Cord Injury Statistical Center, 2023). The primary dangers are immediate and a secondary injury cascade is initiated, resulting in further damage due to swelling and cellular activity changes (Ahuja et al., 2017; U.S. Department of Health and Human Services, 2023b). When SCI at the cervical or thoracic level occurs the autonomic nervous system which maintains homeostasis in the body no longer functions properly. The parasympathetic and sympathetic nervous systems are no longer able to communicate resulting in sympathetic blunting and parasympathetic dominance (Henke et al., 2022). This result may cause individuals with SCI to experience orthostatic hypotension, thermoregulatory dysfunction, respiratory complications, and gastrointestinal dysfunction (Henke et al., 2022; World Health Organization, 2023).

In addition to these complications individuals with high level SCI can experience autonomic dysreflexia (AD), an uncontrolled sympathetic response due to a noxious stimulus below the line of injury (Linsenmeyer et al., 2020). This stimulus is commonly a full bladder but can also be caused by fecal impaction, pressure sores, sunburn or even a too tight shoelace (Cragg & Krassioukov, 2012). Ninety percent of individuals with a high-thoracic or cervical SCI are susceptible to AD and can experience it up to 40 times a day; on average they will experience more than 400 episodes a month (Allen & Leslie, 2023; Linsenmeyer et al., 2020). If AD is not treated quickly and adequately it results in sustained hypertension which can cause organ failure, hemorrhagic stroke, and death (Allen & Leslie, 2023).

AD is a cardiovascular condition resulting from impeded cardiovascular regulation (Sharif & Hou, 2017). During normal cardiovascular autonomic control excitatory and inhibitory afferents are communicated to the nucleus tractus solitarius (NTS) through the vagus and glossopharyngeal nerves. Then the cardiovascular centers receive the information from secondary neurons and create the proper modulatory signals resulting in inhibitory and excitatory efferents being sent to the heart and vasculature (Sharif & Hou, 2017). Impaired cardiovascular function in SCI is the result of the loss of supraspinal control over the sympathetic preganglionic

neurons that control the heart and blood vessels (Sharif & Hou, 2017). Since the spinal and peripheral cardiovascular circuitry below the line of injury are not destroyed, it results in disjointed cardiovascular activities including cardiac arrhythmias and abnormal basal and orthostatic hemodynamics (Sharif & Hou, 2017). As a result of SCI individuals experience an unchanged central venous pressure and a decrease in total peripheral resistance and cardiac output (Grigorean et al., 2009). Case studies have reported patients who experience AD developing atrial fibrillation and other types of arrhythmias without any underlying disease that would predispose them (Pine et al., 1991; Forrest, 1991).

Arrhythmias can be seen in electrocardiograms (ECG) which record the electrical activity that initiates the contractions and relaxations of the heart (Badr et al., 2022). ECG recordings can be collected through non-invasive electrodes which can then be filtered to show skin nerve activity (SKNA) (Doytchinova et al., 2017). These non-invasive electrodes require the animal to be still to record accurately. Radiotelemetry devices allow ECG and blood pressure data to be recorded in free animals more accurately but require implantation surgery (Cesarovic et al. 2011).

The overall objective of this thesis was to understand how autonomic dysreflexia impacts the heart. This was broken down into two main components; understanding how the heart function changes during an AD event and how recurrent AD affects heart function long term, specifically to understand if AD increases the risk of arrhythmias post SCI.

1.2 Research Problem

Spinal cord injury above the T6 level results in a lack of coordination between the parasympathetic and sympathetic nervous systems. This causes dysfunction throughout the body. Negative impacts include autonomic dysreflexia and long-term cardiac changes. However, the specific impact of recurrent AD on cardiovascular system function has not been studied. Understanding how AD affects the changes to heart function seen after SCI can help inform healthcare providers on specifics of what they should be looking for and improve targeted risk prevention of potentially deadly effects of AD.

1.3 Research Questions

For this thesis a rat SCI model was used to investigate physiological parameters as baseline and during autonomic dysreflexia events. The following research questions were addressed:

- 1) Is there a change in QT interval behavior seen during AD events?

Hypothesis: QT interval variability will increase during an AD event.

- 2) Do the ECG parameters RR interval, P wave height, and QRS width change during an AD event?

Hypothesis: An increase in RR interval, P-wave height and QRS width will be seen with noxious stimuli introduction.

- 3) Does AD occurrence cause long term effects in heart function?

Hypothesis: Increased AD occurrence will result in overall decreased heart function and increased risk of arrhythmias.

1.4 Contribution

This thesis focuses on analyzing the ECG parameters R-R interval, P-wave height, QRS width, and QTc interval to understand potential cardiac consequences of recurrent AD. It specifically aims to understand how the risk of arrhythmia is affected by AD events both short and long-term. Understanding how AD affects these parameters would allow individuals to use targeted interventions to reduce the potentially deadly effects of AD.

1.5 Thesis Structure

The first chapter provided a general overview of the problem and information covered in the remaining chapters. Chapter two focuses on the background of the autonomic nervous system and spinal cord injury. Then chapter three focuses on the experimental protocol and data analysis methods used. Chapter four provides the results of direct comparison of the parameters between AD and baseline. Chapter five then goes over the long-term analysis of these parameters. Chapter six, the final chapter, discusses the conclusions, limitations, and future work.

2. BACKGROUND AND LITERATURE REVIEW

2.1 The Autonomic Nervous System

The autonomic nervous system (ANS) regulates the involuntary physiologic processes playing a crucial role in homeostasis. These processes include controlling cardiac muscle contraction, gastrointestinal and bladder functions and regulating blood pressure, heart rate, breathing rate and body temperature (Gordan et al., 2015; McCorry, 2007; Waxenbaum et al., 2022N). The ANS comprises two main interacting components: the sympathetic nervous system (SNS) and the parasympathetic nervous system (PNS). The SNS governs the “fight or flight” response while the PNS governs the “rest and digest” response (Alshak & Das, 2023; Tindle & Tadi, 2022; Waxenbaum et al., 2022). The PNS neurons begin with cranial nerves III, VII, IX, and X as well as sacral spinal roots. The SNS neurons start at the thoracic and lumbar sections of the spinal cord (Patel, 2015). Both systems contain afferent and efferent fibers which receive sensory input and provide motor output (Waxenbaum et al., 2022).

A key component regulating blood pressure are baroreceptors which inform the autonomic nervous system of blood pressure changes on a beat-to-beat basis. Baroreceptors are located in the walls of large system arteries and track the stretch of arteries (Figure 2.1), the higher the blood pressure the more the arteries stretch (Armstrong et al., 2023; Hall, 2021). When blood pressure is changing the baroreceptors transmit more rapidly than they do when the blood pressure is stagnant, relaying excitatory and inhibitory afferents. A rapid decrease in blood pressure results in a decrease in the stretch of the artery wall and a decrease in transmission of the baroreceptors. These signals are transmitted to the tractus solitarius in the medulla, at which point secondary signals excite the medulla’s vagal parasympathetic center and inhibit its vasoconstrictor center (Hall, 2021; Sharif & Hou, 2017). This results in vasoconstriction and increases cardiac output in turn increasing blood pressure (Armstrong et al., 2023).

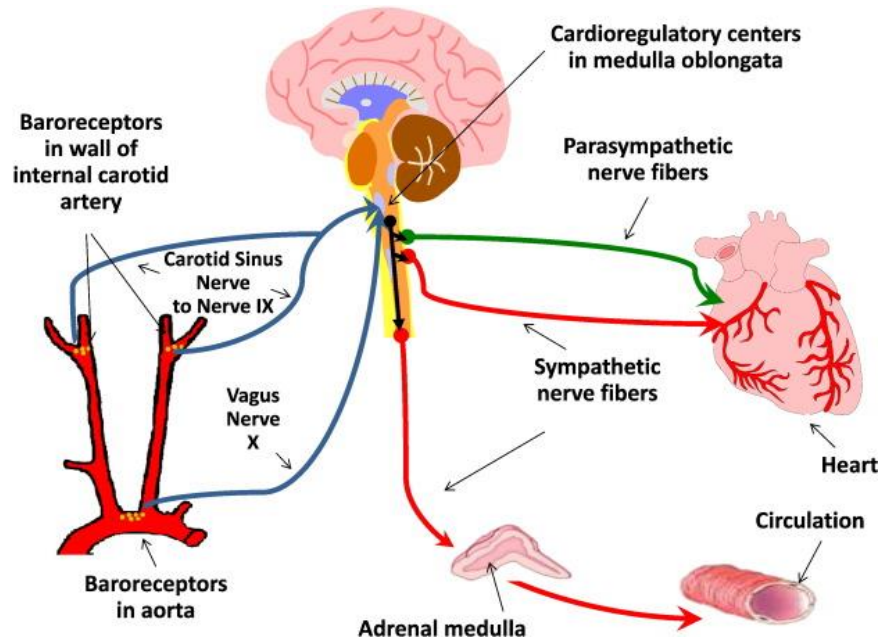


Figure 2.1. Normal autonomic nervous system control of cardiovascular system (La Rovere & Christensen, 2015).

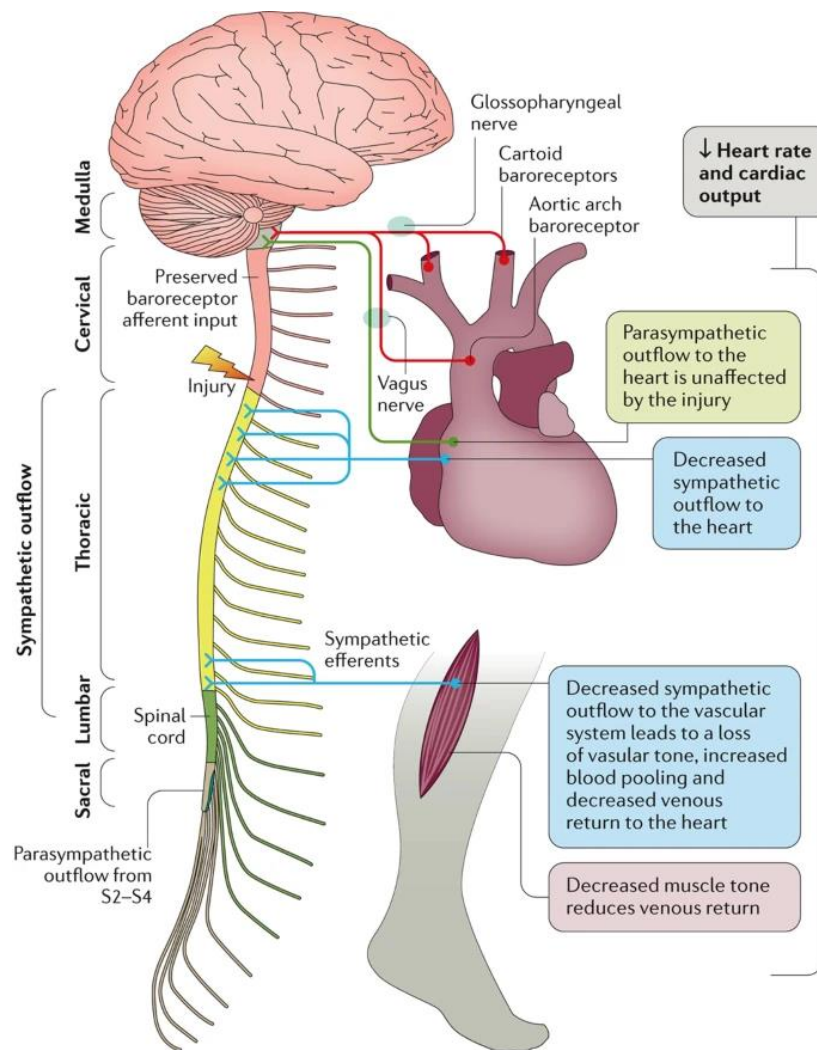
Sympathetic control of the cardiovascular system is mainly noradrenergic (Charkoudian & Rabbitts, 2009). Cardiovascular regulation involves sympathetic preganglionic neurons (SPNs) located between T1 and L2 spinal levels in the intermediolateral cell column of the lateral horn and gray commissure. Those located between T1 and T4 are key as they connect with the sympathetic postganglionic neurons through synapses with the sympathetic chain ganglion (Sharif & Hou, 2017). The SPNs located between T5 and L2 connect to the collateral ganglia then synapse directly to the sympathetic postganglionic neurons. The cardiac sympathetic innervation includes the sinoatrial node, myocardium, and peripheral vasculature. The sinoatrial node stimulation increases heart rate through increasing the slope of diastolic depolarization, the myocardial effects result in an increased stroke volume, and the peripheral vasculature constricts (Charkoudian & Rabbitts, 2009).

Parasympathetic regulation of the cardiovascular system is independent of the spinal cord, acetylcholine acts as a messenger between the pre and postganglionic neurons. The preganglionic neurons synapse with the postganglionic cells which synapse onto the heart (Sharif & Hou, 2017). Parasympathetic regulation of the sinoatrial node results in hyperpolarization of the action potential resulting in a decrease in heart rate. The peripheral vasculature is not directly

affected by the parasympathetic nerves however, they stimulate the release of nitric oxide which causes vasodilation of smooth muscles (Sharif & Hou, 2017).

2.2 Autonomic Dysfunction in Spinal Cord Injury

With a SCI at or above the T6 level the sympathetic and parasympathetic nervous systems are no longer coordinated due to the interruption of neural communication (Wecht et al., 2020). This results in parasympathetic dominance and sympathetic blunting (Figure 2.2). The lack of coordination in regulation between the two systems results in gastrointestinal, genitourinary, thermoregulatory, respiratory, and cardiovascular dysfunction (Henke et al., 2022). It may also result in autonomic dysreflexia, an urgent condition caused by a noxious stimulus (Ahuja et al., 2017).



Nature Reviews | Disease Primers

Figure 2.2. High level SCI effects on cardiovascular system (Ahuja et al., 2017).

Gastrointestinal and genitourinary dysfunction can result in urinary incontinence, inability to empty the bladder, and recurrent urinary tract infections. It may also cause an acute or chronic increase in gastric acid secretions, concomitant constipation, and bowel incontinence (Ahuja et al., 2017; Henke et al., 2022). Due to sympathetic blunting, warm blood from the body's core is not shunted to the periphery for cooling at the surface of the skin and inhibits sweating below the line of injury. In warm environments this can cause neurogenic fever. In cold environments the core temperatures can drop significantly resulting in hypothermia (Henke et al., 2022). Respiratory complications are the number one cause of death in people with chronic SCI (Ahuja et al., 2017). Parasympathetic dominance leads to bronchiolar constriction, increased

mucus secretion, and hyper-reactive airways. SCI also results in ineffective cough and increased fatigue which can cause recurrent pneumonia and mucus plugging (Ahuja et al., 2017; Henke et al., 2022).

Orthostatic hypotension is a common result of the compromised sympathetic outflow caused by SCI (Ahuja et al., 2017). Orthostatic hypotension occurs when blood pressure drops suddenly when moving to a standing position, symptoms include dizziness, nausea, and syncope (U.S. Department of Health and Human Services, 2023a). Other results of cardiovascular dysfunction include neurogenic bradycardia, risk of AV block, diminished venous vascular tone, and adaptive myocardial atrophy (Henke et al., 2022).

For patients with injuries at or above the T6 level autonomic dysreflexia (AD) poses a potentially deadly problem, increasing risk of stroke by 300 to 400 percent (Allen & Leslie, 2023). Autonomic dysreflexia is a sudden increase of at least 20 mmHg in systolic blood pressure caused by a noxious stimulus below the line of injury (Harvey, 2008). Significant episodes of AD see a blood pressure increase of at least 40 mmHg. Common noxious stimuli that can trigger AD include urinary tract infections, distended bladders, and fecal impaction (Allen & Leslie, 2023; Cragg & Krassioukov, 2012; Harvey, 2008). The initial symptom of AD is often a severe headache, other symptoms include sweating in the lower part of the body, facial flushing, and bradycardia (Allen & Leslie, 2023). The noxious stimulus excites neurons in the sympathetic chain resulting in unchecked reflex responses. This results in diffuse vasoconstriction below the level of injury causing a significant blood pressure increase. Above the level of injury, the parasympathetic system responds with vasodilation; however, it is unable to compensate for the vasoconstriction below the level of injury (Allen & Leslie, 2023; Harvey, 2008).

2.3 Prevalence of SCI and Autonomic Dysreflexia

Between 250,000 and 500,000 SCIs occur around the world every year (World Health Organization, 2023). Out of the developed regions North America has more incidences of traumatic spinal cord injury than Australia or Western Europe with approximately 18,000 new cases a year (Ahuja et al., 2017; National Spinal Cord Injury Statistical Center, 2023). Vehicle crashes and falls are the most common cause of traumatic SCI, violence is also a common cause, it, and self-harm account for the increased incidence in North America. Seventy-nine to eighty percent of new traumatic SCI cases are male with the greatest incidence occurring between ages

15 to 29 and as the older population grows and increase in SCI is seen in the population over 60 years of age (Ahuja et al., 2017; National Spinal Cord Injury Statistical Center, 2023). Premature death is two to five times more likely in individuals with SCI (World Health Organization, 2023). One of the most common causes of death is cardiovascular disease which can be caused by abnormal blood pressure control (Lee & Joo, 2017).

Autonomic dysreflexia is one condition resulting in abnormal blood pressure control and an increase in sympathetic activity as measured by skin nerve activity bursts (Kirby, 2022). AD commonly occurs in individuals with injury at the T6 level or higher and can be triggered by noxious stimuli such as distended bladders and fecal impaction (Ahuja et al., 2017; Allen & Leslie, 2023). In a study of 28 individuals, it was found that the incidence rate of asymptomatic AD was 42.9 percent with an overall AD incidence of 92.8 percent (Lee & Joo, 2017). Another study of 571 patients found that 24.7 percent of patients were diagnosed with asymptomatic AD. The incidence rate of AD was the greatest in patients who used reflex voiding as their bladder emptying method while those who used continent spontaneous voiding had the lowest rate of AD (Furusawa et al., 2011). With life threatening complications it is important that AD is prevented long term and quickly detected and treated when it does occur. With a high incidence of asymptomatic AD, it is important that all individuals with SCI are monitored and aggressively diagnosed (Ahuja et al., 2017; Lee & Joo, 2017).

2.4 Impacts on the Heart and QT Interval

SCI is associated with an increased risk of cardiovascular disease and chronically alters the structure and function of the cardiac system. Sympathetic blunting results in altered cardiac loading and reduced inotropic function resulting in reduced cardiac output and left ventricular volume (Fossey et al.,2022; Henke et al., 2022). In addition, after initial injury 60 percent of SCI patients experience consistent orthostatic hypotension which for most patients gradually resolves within a few months (Ahuja et al., 2017). Other cardiac complications that may occur include cardiomyocyte atrophy and reduced left ventricle contractility (Fossey et al.,2022).

Individuals with cardiovascular disease show increased mortality with QT interval prolongation (Diedrich et al., 2002). The QT interval represents the duration of ventricular activation and recovery (Ambhore et al., 2014). QT interval prolongation is associated with syncope, cardiac arrest, and lethal arrhythmias including torsade de pointes (Al-Akchar &

Siddique, 2022). The variability of the QT (QTV) interval measures the fluctuation in QT interval duration and shows cardiac electrical instability (van den Berg et al., 2019). Increased QTV is a predictor of malignant ventricular arrhythmia including frequent ventricular fibrillation (Baumert et al., 2011; Bigger, 1983).

SCI does not always result in cardiovascular disease but may still result in changes to the QT interval. Studies have shown that individuals with an SCI level \leq T6 had longer QT and QTc intervals and an increased incidence of QT prolongation during the acute phase (defined as within 24 hours of injury) compared to the chronic phase of SCI (1 year after injury). QT prolongation can predict occurrence of torsades de pointes (Isoda & Segal, 2003). For individuals with an injury $>$ T6 there were no significant differences in electro cardiac parameters (Chung et al., 2011). They also found that the QTc could be used to predict mortality, and individuals who died within 30 days of injury had longer QT and QTc intervals (Chung et al., 2011). Other studies have shown that while individuals with SCI have cardiac autonomic control differences when comparing individuals with low level SCI (T6 and below) with controls of the same age and gender there was no significant difference in QTc (Heffernan et al., 2007).

A retrospective cohort study found that chronic SCI is associated with an increased risk of atrial fibrillation (Forrest, 1991; Wang et al., 2016). Case studies have reported that risk of atrial fibrillation may be increased by autonomic dysreflexia (Pine et al., 1991; Forrest, 1991). One of which proposed that the patient's atrial fibrillation was induced by an autonomic dysreflexia event (Pine et al., 1991). However, there has not been a study that directly links AD to atrial fibrillation.

3. ANIMAL MODEL

3.1 Model Selection

In SCI research 72% use rat models and 81% study thoracic SCI (Sharif-Alhoseini et al., 2017). Sprague-Dawley outbred rats are extensively used for animal models of various conditions including cardiovascular diseases and SCI (Mestre et al., 2015; Brower, 2015). The majority of SCI studies use Sprague-Dawley rats (Akhtar et al., 2009).

Due to their outbred nature, they also have interindividual genetic variation seen in humans (Banek et al., 2021). Rats are also preferred models of SCI as mice models show cell proliferation at the site of injury, lack cyst formation, and some regeneration even with a complete transection of the spinal cord. Humans and rats both commonly develop cysts, formation of fibrotic tissue at lesion site, and with a full transection do not exhibit regeneration (Kjell & Olson, 2016). The use of Sprague-Dawley rats over human models allows for greater experimental control including diet, light, and temperature. Rat models also allow for a larger sample size (U.S. Department of Health and Human Services, 2022).

The ability to use internal implants in the rats also offers the advantage of accurate cleaner signal collection (Konopelski & Ufnal, 2016). This results in an ECG where features are easier to extract for analysis. This study used the HD_S11_F0 radiotelemetry implant from Data Sciences International to record blood pressure, heart rate, body temperature, and ECG. The implant has a sampling frequency of 1 Hz with a two-month battery life (AD Instruments, n.d.). The implant works the Ponemah® program to record and analyze the detected information. For the purposes of this study the automatic calculation of heart rate, RR interval, P-wave height, and QRS width which Ponemah® provides through the implant software were used. The QT interval was independently calculated due to difficulty detecting the T-wave. These parameters were able to be calculated from ECG to provide insight on how the heart is functioning. RR interval is the reciprocal of heart rate. While P-wave shows the atrial depolarization and the QRS complex is the ventricular depolarization (Ashley & Niebauer, 2004). The QT interval shows ventricular systole (Ambhore et al., 2014).

The use of external electrodes allows for the filtering and analysis of skin nerve activity (SKNA). SKNA activity is a way to measure sympathetic nerve activity and can be used to

estimate sympathetic tone (J. Chen et al, 2021; Everett et al., 2017;). Kirby showed that SKNA features increased during AD before an increase in blood pressure was seen and were significantly different between AD and baseline events (Kirby, 2022). SKNA bursts are sudden increases in nerve activity and are associated with an increased short-term variability of the QT interval (S. Chen et al., 2021).

3.2 Implant Surgery

To implant the radiotelemetry device before arrival to the Purdue research lab, Data Science International (DSI) trained staff used rats weighing between 350 and 400g. During this procedure the HD_S11_F0 implant (DSI, USA) was placed in the intraperitoneal cavity with abdominal cannulation. The electrodes were placed in a modified Lead II configuration. The catheter was inserted between the renal arteries and iliac bifurcation in the abdominal aorta and the implant suture rib was incorporated into the abdomen wall closure. Before being sent to the research lab the rats had 5 days of recovery time ('HD-S Device Surgical Manual', n.d.).

3.3 Acclimation

Upon arrival at Purdue the rats were housed individually in plexiglass cages with straw bedding; they had access to food and water. For the first 2 days at the facility the rats were left to acclimate to their environment. After acclimation to their new housing environment the rats began the 4-week acclimation protocol (Kirby et al., in press). This protocol had 3 main phases, 1-acclimation to researchers, 2-acclimation to restraint, and 3-acclimation to sensors (Figure 3.1).

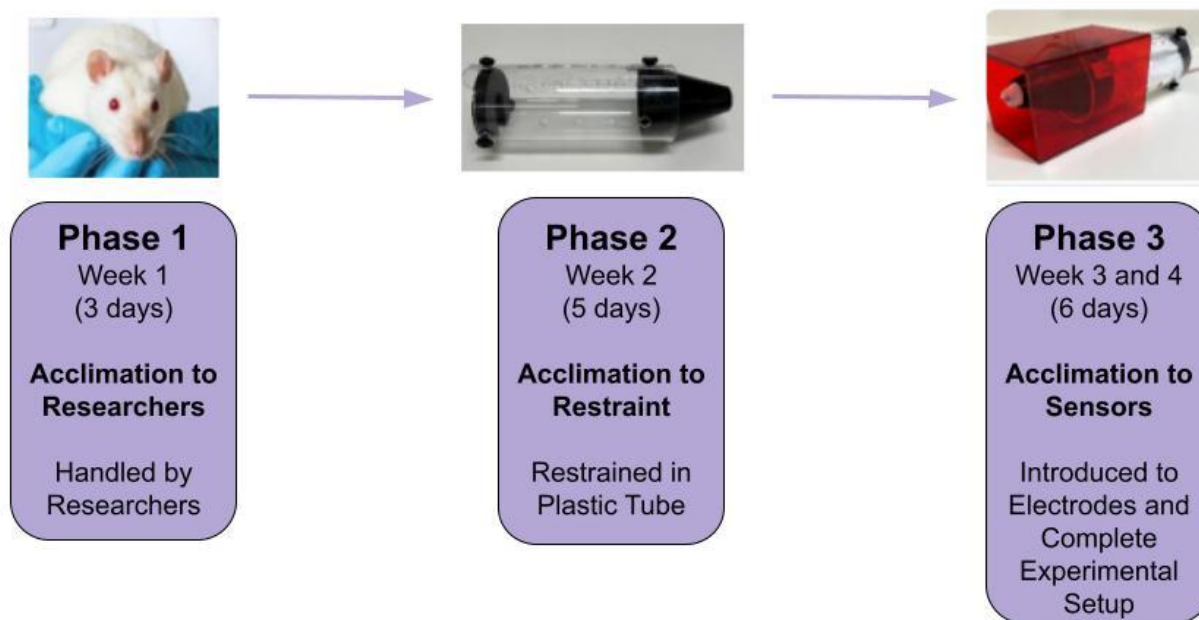


Figure 3.1. Acclimation protocol phases.

During the first week of acclimation the rats were introduced to the researchers starting with 10 minutes at a time and increasing to 20 minutes over three days. Researchers stuck their hand in the cage and when the rats began to feel more comfortable initiated contact and tickling (Cloutier, 2018). This allowed the rats to become familiar with the scent and sounds of the researchers. Care was taken for researchers to maintain a similar smell throughout the entirety of the protocol. During this time the rats were also introduced to the restraint tube which was placed in their cage for them to explore. After each session the rats were rewarded with peanut butter.

In the second week of acclimation (Phase 2) the animals were acclimated to their restraint. They were restrained in the tube once a day starting at one minute, the next day was five minutes then 10,15, and finally 30 minutes which was hit on day 14 from arrival to Purdue’s facility.

The third phase consisted of two weeks. The first week the rat was introduced to the electrodes and during the second week the rat was introduced to the entire experimental set up. During the third phase acclimation occurred every other day to reduce isoflurane exposure and minimize the development of aversion to gas anesthesia. For electrode introduction the rats were anesthetized with 4% isoflurane. The chest and lower right leg were then shaved, and Nair was used to ensure that hair was fully removed, 70% ethanol was used to clean these areas. The

electrodes were placed in a Lead I configuration using conductive gel. To ensure the electrodes stayed in place the top ones were held by a piece of cloth and Velcro and the bottom one was held with medical tape. The rat was then placed into the restraining tube. In week four the alligator clamps and rodent snuggle were introduced. The snuggle was used to restrict movement and help keep the electrodes secure. They were acclimated to the entire experimental set up starting at 10 minutes increasing to 50 minutes over four days through the course of the week.

3.4 High Thoracic Spinal Cord Injury Surgery

After completion of the acclimation protocol the rats underwent a high thoracic spinal cord injury surgery. They were anesthetized with 4% isoflurane, shaved at the surgical site, cleaned with povidone iodine solution then placed on a heating pad using a tube to accentuate the guide bone. To confirm sedation a toe pinch was used and then anesthesia was reduced to 2% isoflurane. They were administered Ethiqva (.1mL/200g SC), Meloxicam (1-2mg/kg SC), and Baytril (9.1mg/kg SC). The rat was then draped under aseptic conditions (Squair et al., 2017) The spine was exposed through a T1 - T5 midline incision. At the T3 level a laminectomy was performed, exposing the spinal cord. Standardized forceps with 1.2mm thickness were used for 15 seconds to compress the spinal cord. The injury was verified by visually inspecting for clotting patterns which would appear as a dark red line across the spinal cord. Once the injury was complete the incision was closed with 4-0 prolene sutures, the area was cleaned with 70% ethanol and triple antibiotic cream was applied over the sutures.

3.5 Post SCI Care

Once surgery was complete the rat's bladder was manually expressed and 15mL of lactated ringer solution was administered subcutaneously. The rats remained on the heating pad and monitored until they were fully aware and awake. To confirm injury completion a toe pinch was used. During this time a cage was prepped with ALPHA-dri(r) bedding to prevent abdominal irritation, peanut butter, applesauce, Ensure and water to promote eating as SCI can result in weight loss.

For the following three days the rats were administered Meloxicam and Baytril once a day to reduce pain and prevent infection. If it was deemed necessary by the veterinarian,

administration of these drugs continued. For the first 10 days post op, the rats had their bladders manually expressed three times a day after which it was reduced to as needed. For all 21 days post SCI injury the rats had their food changed and were weighed and monitored by trained personnel. If animals lost more than 20% of their pre-op body weight, they were euthanized (Ramsey et al., 2010).

3.6 Sensors

To collect data from the HD-S11-F0 implant the restrained rat or rat cage were placed on top of a receiver and turned on using a magnet. Ponemah ® Software (*DSI, USA*) was used to acquire and summarize the real time blood pressure and ECG data collected from the implants. The data was collected at 1kHz. Once data collection was completed the implants were turned back off with the magnet to preserve their battery life.

For non-invasive data collection, disposable gel-based electrodes were placed in a Lead I configuration (Figure 3.2a). The electrodes were secured using a snuggle (Figure 3.2b). These electrodes were connected to a bio-amplifier on the Power Lab 26T (*AD Instruments, USA*) and data was collected at 10kHz. The data was bandpass filtered at 500 – 1000 Hz to extract SKNA.



Figure 3.2. (a) Lead I placement of external electrodes and (b) External electrodes, alligator clamps, and snuggle.

3.7 Induction of AD

Colorectal distension mimics visceral pain in humans and is a widely used noxious stimulus in autonomic dysreflexia studies imitating fecal impaction (Hou et al., 2014; Jaffe & Thompson, 2015; Krassioukov & Weaver, 1995; Ness & Gebhart, 1988; O’Mahony et al., 2012).

CRD experiments started on day 5 post SCI surgery. The rat was first anesthetized with 4% isoflurane. The external electrodes were placed along with alligator clamps (1 under their

right front limb and one at their left bottom limb). A balloon inflated catheter was then lubricated and placed 2 centimeters into the rectum. The rat was then wrapped in a snuggle and placed in a restraining tube (Figure 3.3). They were then put on the receiver and given 20 minutes to wake up and acclimate before inflating the balloon with 2 mL of air.



Figure 3.3. Experimental setup with external electrodes, alligator clamps, snuggle, restraint tube, blackout box, and foley catheter.

As ECG data was simultaneously recorded by the implant and external electrodes the alligator clips were used to deliver a 1 Volt single square pulse generated by a GRASS s48 Stimulator to align the signals. The clips were attached to the stimulator using a coax cable. A button on the stimulator was used to initiate the pulse at the recorded time which also initiated the inflation of the balloon catheter. For consistent inflation force and time, a 3D printed syringe holder with a small motor was used (Figure 3.4). Inflation of the balloon occurred three times in each experiment with 11 minutes between each initiation. The balloon stayed inflated for one minute and then 10 minutes of recovery time was given. This experiment occurred on days 5,7,9,11,14,16,19 and 21 post SCI surgery.

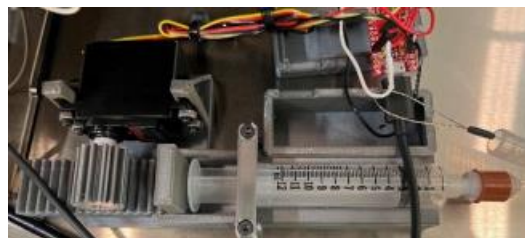


Figure 3.4. 3D printed syringe holder for catheter inflation.

3.8 Signal Processing

An AD event occurred when an increase of 15 mmHg from the mean systolic blood pressure recorded by the implant was detected (Suresh et al., 2022).

Files were excluded from analysis due to excessive noise or saving failure.

The external electrode ECG was digitized at 10 kHz, and bandpass filtered from 500 to 1000 Hz to extract the SKNA features. This was then down sampled to 2 kHz and then integrated over 100 ms in MATLAB to get the integrated SKNA (iSKNA). To find where bursting occurred a dual threshold algorithm was applied. When the iSKNA amplitude passed the first threshold the start of the burst was defined and when it passed the second lower threshold the end was defined (Cole et al., 2019). Detected bursts can be seen as the red in Figure 3.5.

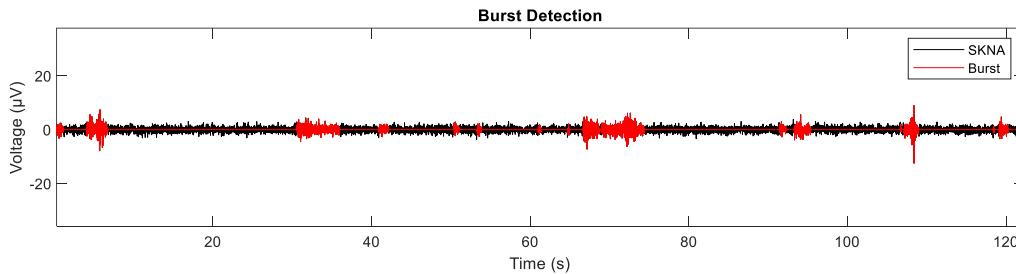


Figure 3.5. Burst detection example. Bursts are represented by the red sections.

Detection of the T-wave in noisy conditions is difficult (Tiwari, 2021; Vazquez-Seisdedos et al., 2011). To detect the T-peak the ECG was Savitzky-Golay filtered, and S-peak was found using a wavelet transformation, with a defined peak prominence and height (Hargittai, 2005; Bsoul et al., 2009). The overall peaks were detected again, those that appeared immediately after the detected S-peaks were labeled at T-peaks. To detect the Q-peak the R peak was found through taking the sections between each detected S-peak and finding the first location where the derivative changes sign going backward through the signal. This same method was used for finding the Q-peaks based on the R-peak locations; that point was then shifted to the local minimum. All detections were verified by hand. Peak detection results can be seen in Figure 3.6.

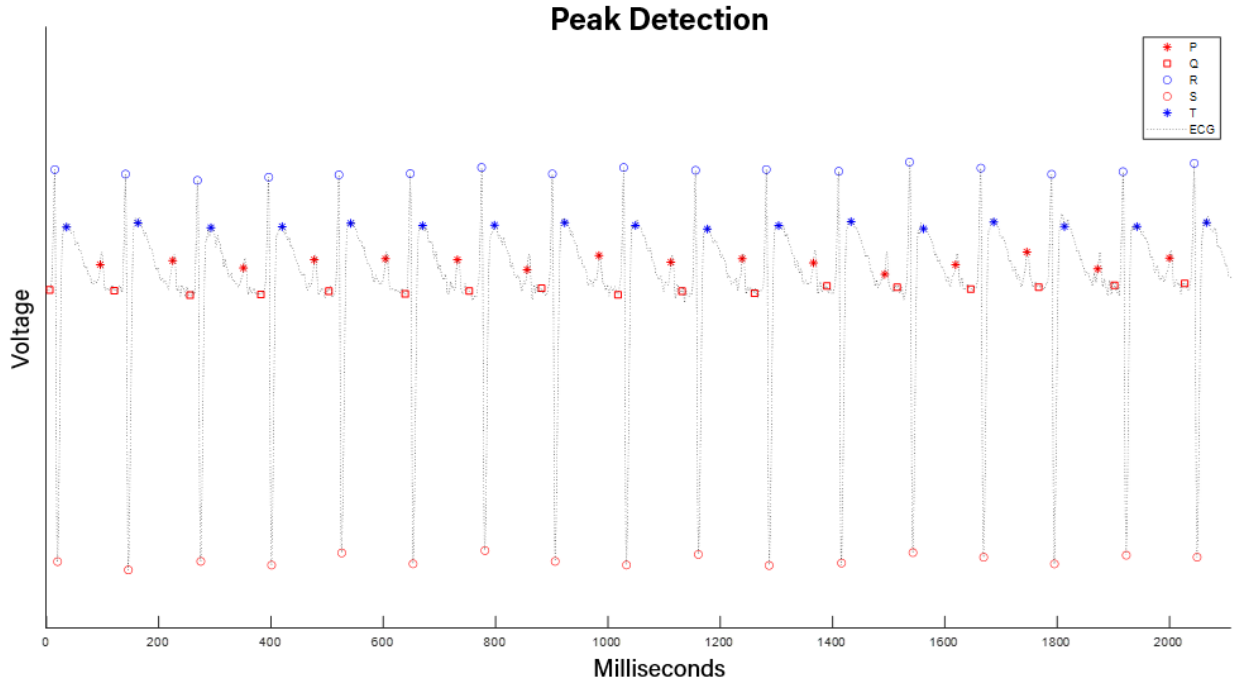


Figure 3.6. Peak detection results.

The tangent method was then used to determine the end point of the T-wave (Figure 3.7) (S. Chen et al., 2021). The QT interval was calculated by taking the T-wave end point of each heartbeat and subtracting the Q-peak. As QT interval varies with heart rate it was corrected using a normalized Bazett's formula $QT_c = QT / \sqrt{RR/f}$, $f = 135$ (Kmecova & Klimas, 2010). Short term variability of the QTc interval (STVQTc) was calculated using:

$$STVQT_c = \frac{\sum_{n=1}^{30} |QT_{n+1} - QT_n|}{30\sqrt{2}} \text{ (Baumert et al., 2016; S. Chen et al., 2021).}$$

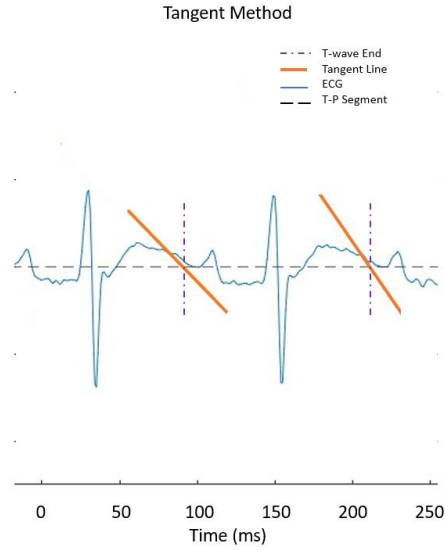


Figure 3.7. Tangent method of finding the T-wave end point for QT calculations.

All other ECG parameter values were taken from the automatic calculations in Ponemah®. All signals were synchronized using a 1-volt square wave pulse. These values were lined up to the 1-volt shock removing the data immediately around it, removing the non-physiological outliers at this location (Figure 3.8).

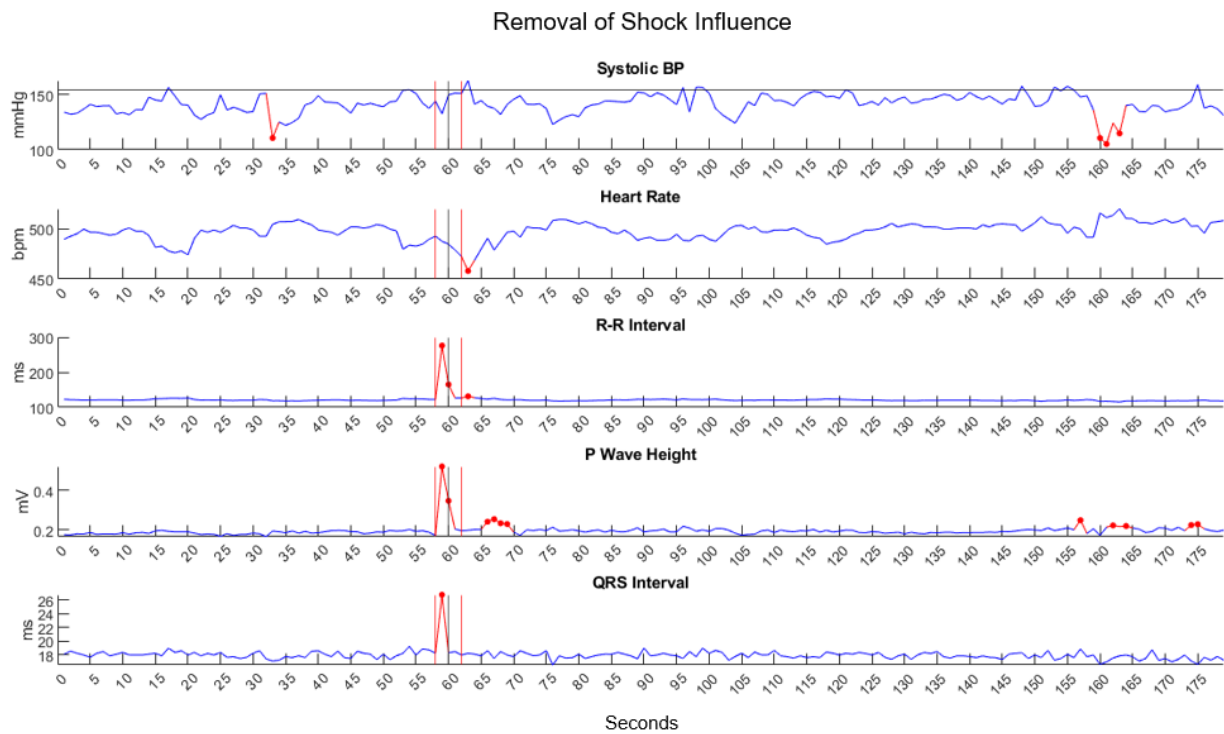


Figure 3.8. Removal of calculated values influenced by 1-volt shock. The vertical red lines which surround the vertical black line represent the start and end points of data removal due to the 1-volt shock.

4. GENERAL BEHAVIORS

Over the course of experimentation, a total of 128 AD events were triggered through CRD in 10 rats. On average each rat experienced 12.8 events overall or 1.6 events on each trial day ranging from a total minimum of 5 events to a maximum of 22 AD events.

4.1 Autonomic Dysreflexia vs. Baseline

An ANOVA with a Tukey Kramer Post-hoc Test showed that the QTc interval and STVQTc were significantly different between baseline and AD events ($p < 0.05$). The average baseline QTc interval was $52.32 \pm .08$ ms while for AD it was significantly longer at $52.49 \pm .06$ ms (Figure 4.1). AD also resulted in an increased STVQTc at $8.12 \pm .01$ ms while baselines was $7.85 \pm .01$ ms (Figure 4.1).

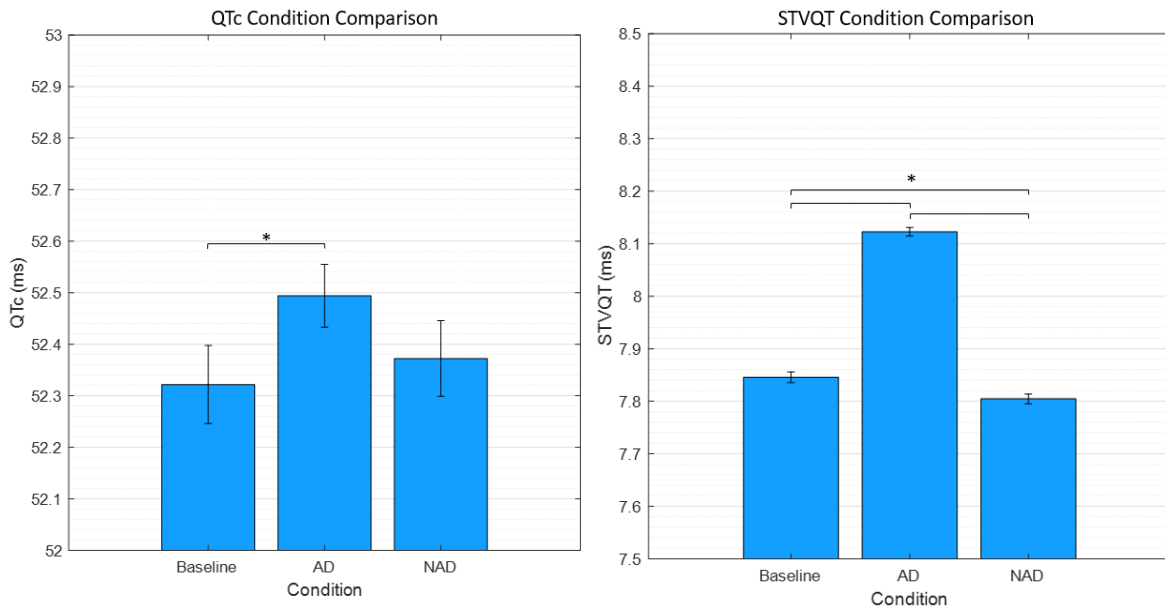


Figure 4.1. Comparison of QTc and STVQTc for baseline, AD, and non-AD (NAD) conditions (* $p < 0.05$).

For comparison of systolic blood pressure, RR interval, P-wave height, and QRS width values between baseline and AD events paired t-tests were used. The sustained systolic blood pressure significantly increased for the duration of AD events (152.67 ± 1.11 vs. 155.09 ± 1.12 mmHg) 97 of 118 AD events resulted in an increase ($p < 0.05$). AD events did not result in a

significant change in RR interval or heart rate (66 events had an increase in heart rate and 52 showed a decrease). During AD p-wave height significantly increased from 0.143 ± 0.006 to 0.146 ± 0.006 mV, 66 events had an increased in P-wave height, the increases were greater than the 52 events which resulted in minimal increases. QRS width decreased from 19.22 ± 0.14 to 19.12 ± 0.14 ms during AD events, only 37 of the 118 events resulted in an increase in QRS width ($p < 0.05$)(Figure 4.2).

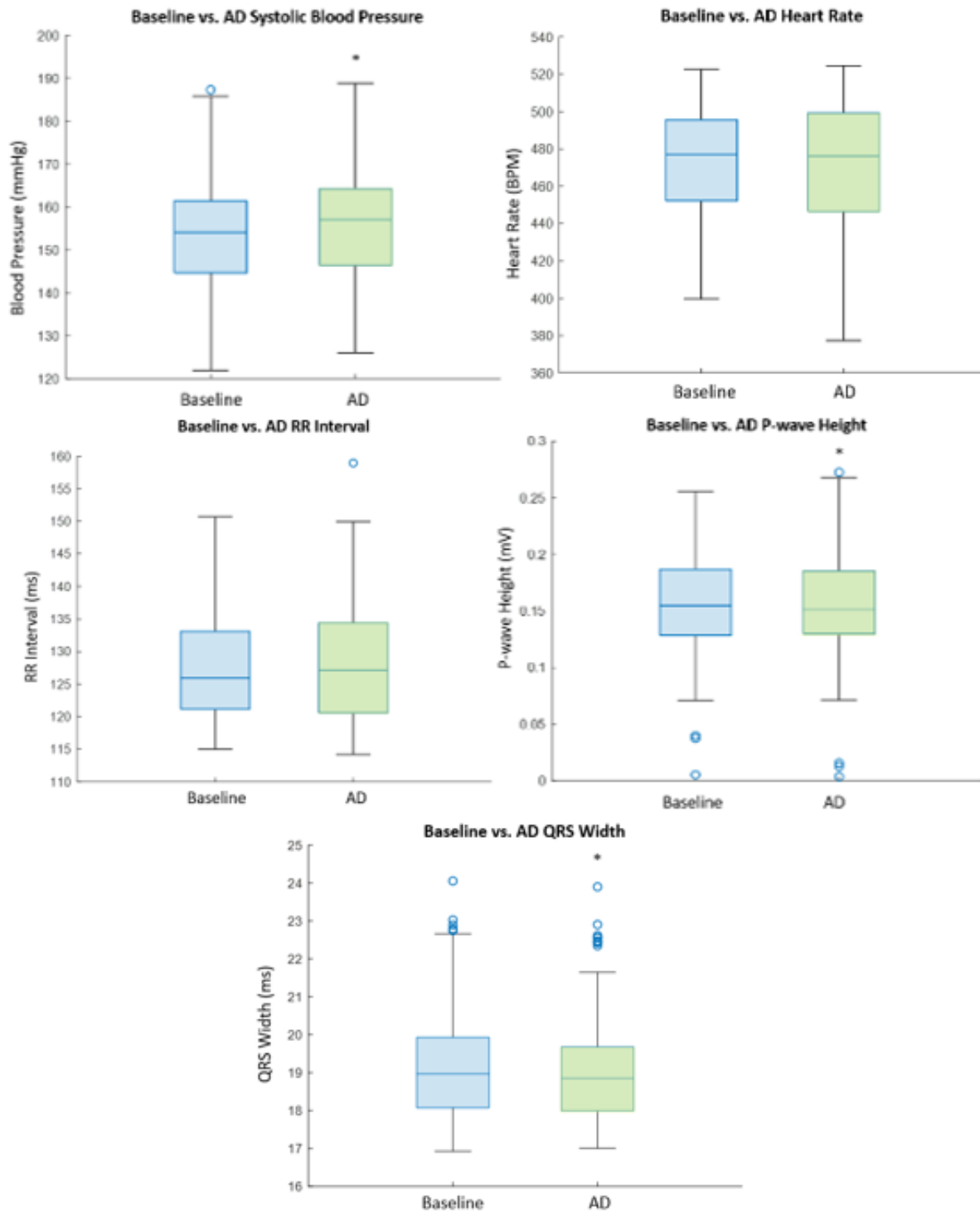


Figure 4.2. Baseline vs. AD comparisons (N = 10 rats) (*p < 0.05). Blood pressure, P-wave height, and QRS width were significantly different between AD and Baseline.

4.2 SKNA Bursting Activity

SKNA bursting activity was detected through a dual threshold algorithm where the iSKNA must first pass a higher boundary to start counting as a burst and when it passes a second lower threshold the burst ends (Cole et al., 2019). It can also be visualized as spikes in iSKNA. When these spikes are seen a peak in QT interval variation is also noticed (Figure 4.3).

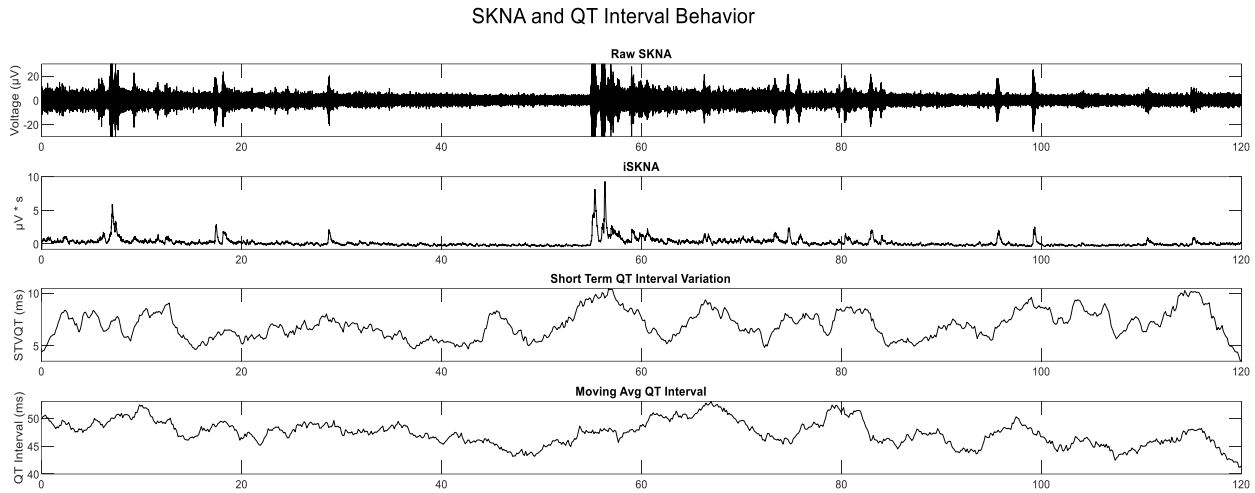


Figure 4.3. SKNA bursting activity with QTc behavior.

During SKNA bursting activity there was a significant increase in QTc ($52.55 \pm .03$ ms to $53.60 \pm .05$ ms) (Figure 4.4) and in STVQTc ($7.99 \pm .004$ ms to $8.03 \pm .007$ ms) (Figure 4.5) ($p < 0.05$).

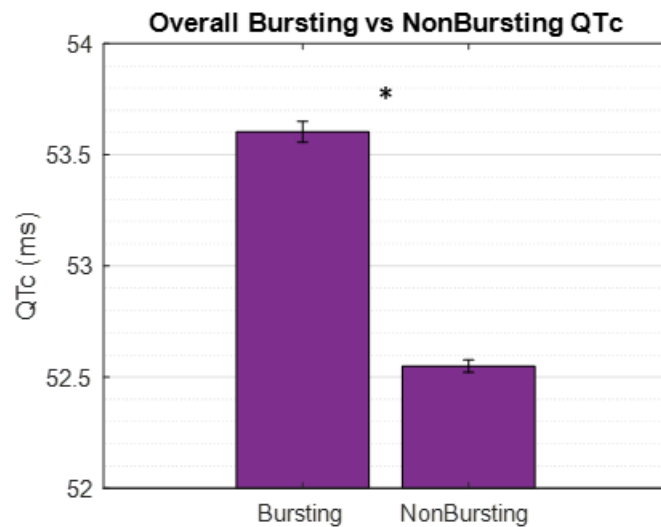


Figure 4.4. Comparison of QTc during SKNA bursting and non-bursting (N = 10 rats) (* $p < 0.05$).

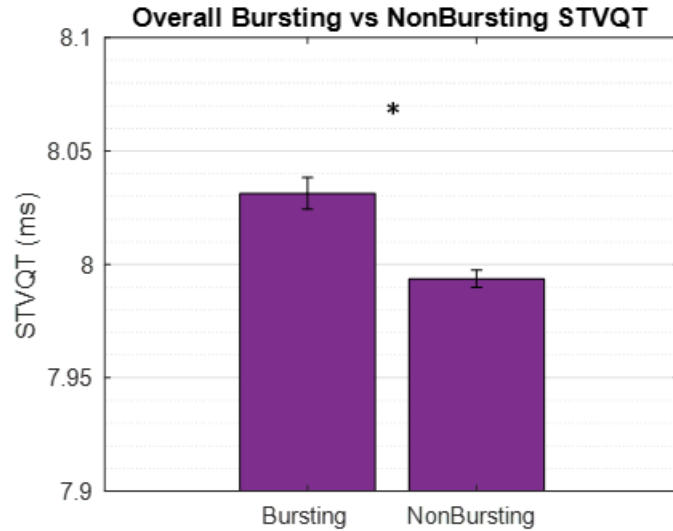


Figure 4.5. Comparison of STVQTc during SKNA bursting and non-bursting (N = 10 rats) (*p < 0.05).

4.3 Overall Insights

AD prolonged both the QTc and STVQTc when compared to baseline. This was also seen during bursting activity. It has been reported that bursting activity is increased during AD events, it is possible that the differences seen during AD events are due to an increase in SKNA bursting activity overall (Kirby et al., in press). The increase in QT interval short term variability may result in an increased risk of ventricular arrhythmias during an AD event (Smoczynska et al., 2020).

The increase in overall systolic blood pressure during AD as a spike of 15 mmHg or greater was used as the gold standard for detecting AD in the rat model (Suresh, Everett IV, et al., 2022). While heart rate and RR interval did not have any significant change from baseline to AD events Suresh et al. (2022) reported that including heart rate in the detection algorithm for AD along with galvanic skin response and skin temperature increased accuracy. The overall lack of significant difference was consistent with previous findings that heart rate is not consistently bradycardic or tachycardic during AD (Suresh & Duerstock, 2020).

P-wave height was used as an indicator of right atrial enlargement (Harrigan, 2002). The significant increase in P-wave height during an AD event may be the result of increased right heart strain during AD (Douedi & Douedi, 2022). The QRS width was significantly shorter during AD events, a short QRS is a marker for increased risk of arrhythmia (Wolpert et al., 2008).

Overall the increased QTc and STVQTc combined with the shortened QRS width, indicated that there may be an increased risk of arrhythmia during AD events.

5. LONG TERM CHANGES IN CARDIAC PARAMETERS

After spinal cord injury there are two different pathological events occurring during subacute and chronic time periods. During the subacute phase of injury there is sodium dysregulation which causes excitotoxic neuronal cell death propagating the secondary injury cascade. In the chronic phase of injury, the initial inflammatory response diminished and remodeling of neural circuits, vascular reorganization, and remyelination commences (Ahuja et al., 2017). The subacute phase of injury is defined in prior research as day 5 through day 11 (Martín-López et al., 2021). The chronic phase is defined as day 14 through day 21.

5.1 Blood Pressure Behavior and AD Incidence

The incidence of AD increased during the subacute period (day 5 – 11), it then dropped on day 14 to increase again as throughout the chronic phase (day 14 – 21) (Figure 5.1).

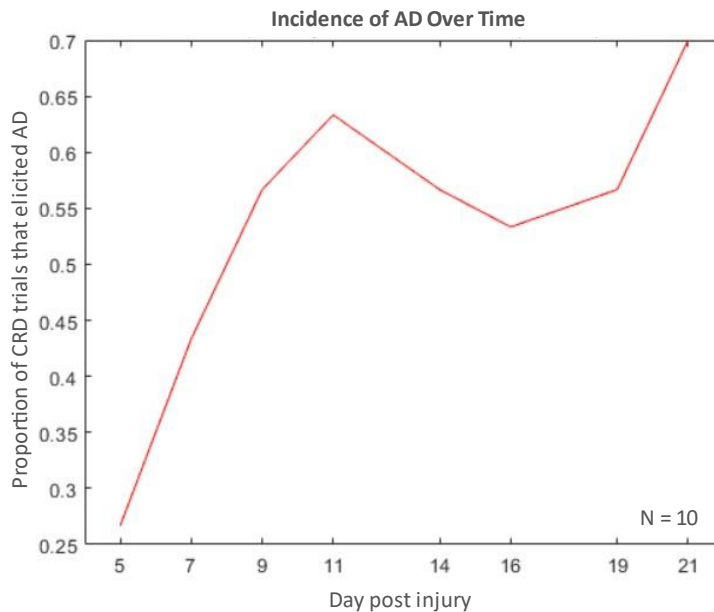


Figure 5.1. AD incidence across the 21 days post injury (N = 10).

During the subacute phase of SCI, the amount that blood pressure spikes above the mean during AD events consistently decreased. During the chronic phase this spike above the mean

blood pressure increased; however, there are only significant differences between day 5 and day 14, and day 5 and day 21 (Figure 5.2). A similar pattern is seen in the total amount of blood pressure spikes above the AD threshold throughout the event, none of these differences are significant (Figure 5.3).

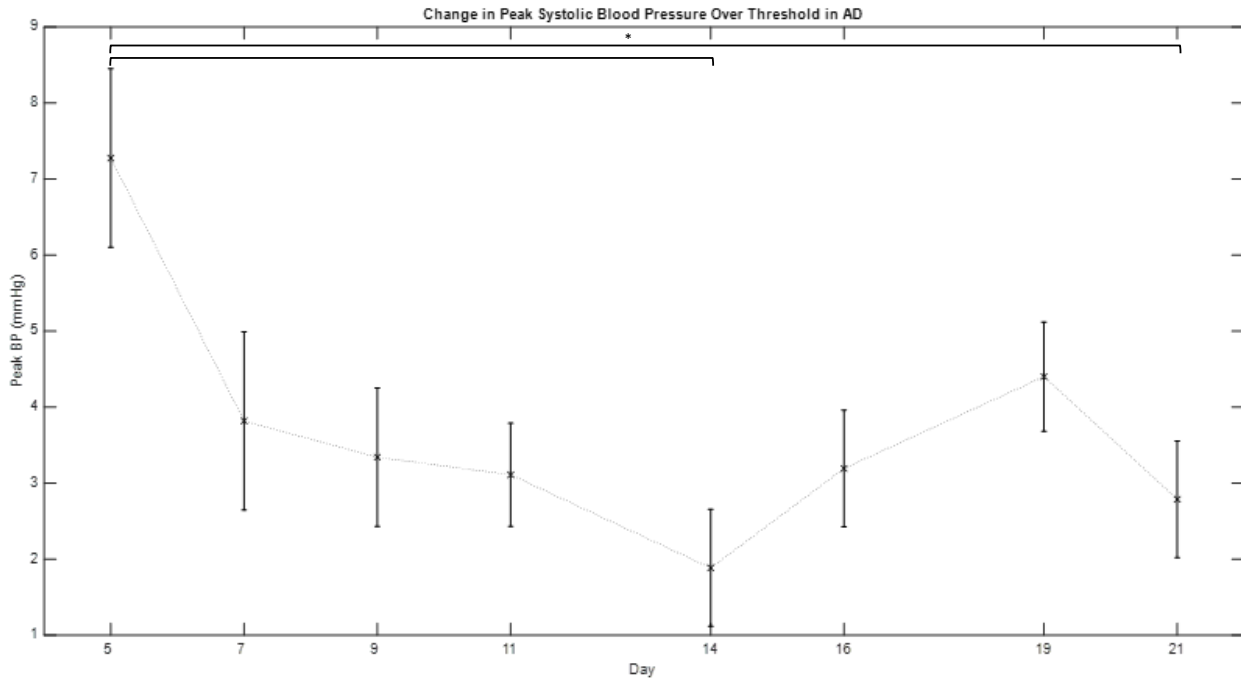


Figure 5.2. Systolic blood pressure peak value above threshold during AD events (* $p < 0.05$).

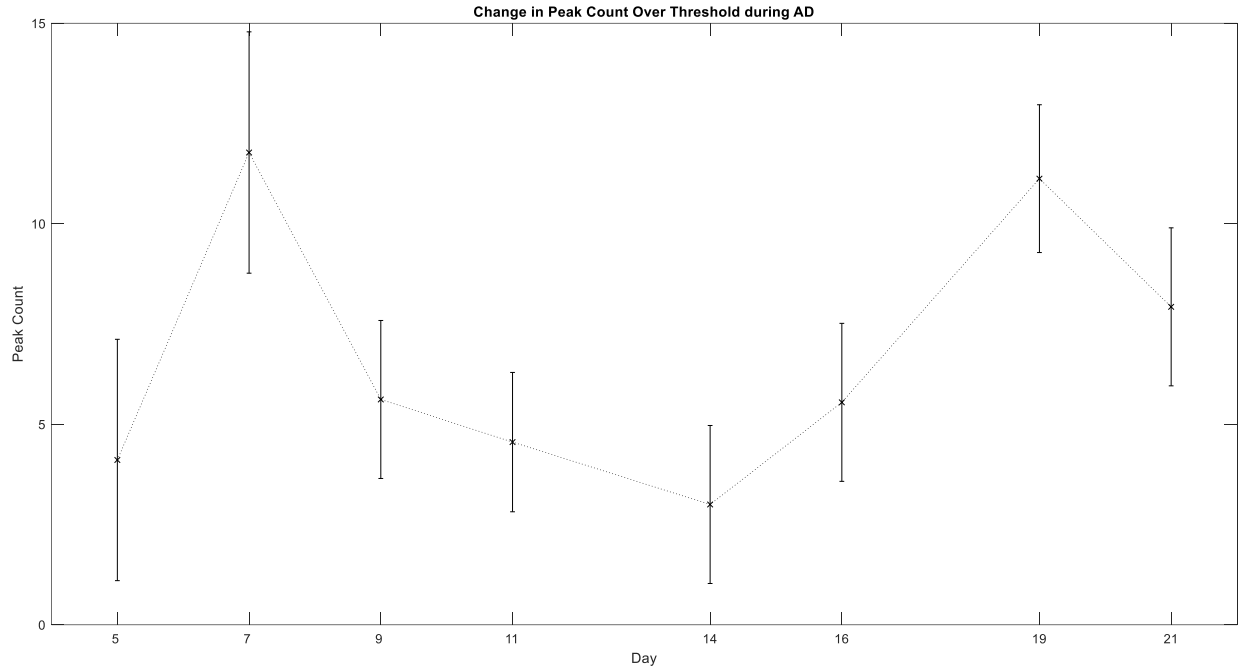


Figure 5.3. Peak above threshold count during AD events.

5.2 ECG Components and Observations

During the subacute phase of injury (day 5 - 11) the baseline QTc increased significantly from $51.56 \pm .28$ ms to $53.08 \pm .28$ ms ($p < 0.05$), the AD QTc followed a similar pattern from $48.79 \pm .30$ ms to $52.68 \pm .20$ ms ($p < 0.05$). Both groups experienced a peak in QTc on day 9 with means of 53.81 and 55.34 ms respectively ($p < 0.05$). This change was not seen in the CRD trials that did not result in AD (NAD), instead a significant decrease in QTc was seen from $53.07 \pm .21$ ms to $51.82 \pm .34$ ms ($p < 0.05$) (Figure 5.4). The QTc increased during both bursting and non-bursting SKNA ($p < 0.05$). This increase corresponded with the increase in AD susceptibility over time.

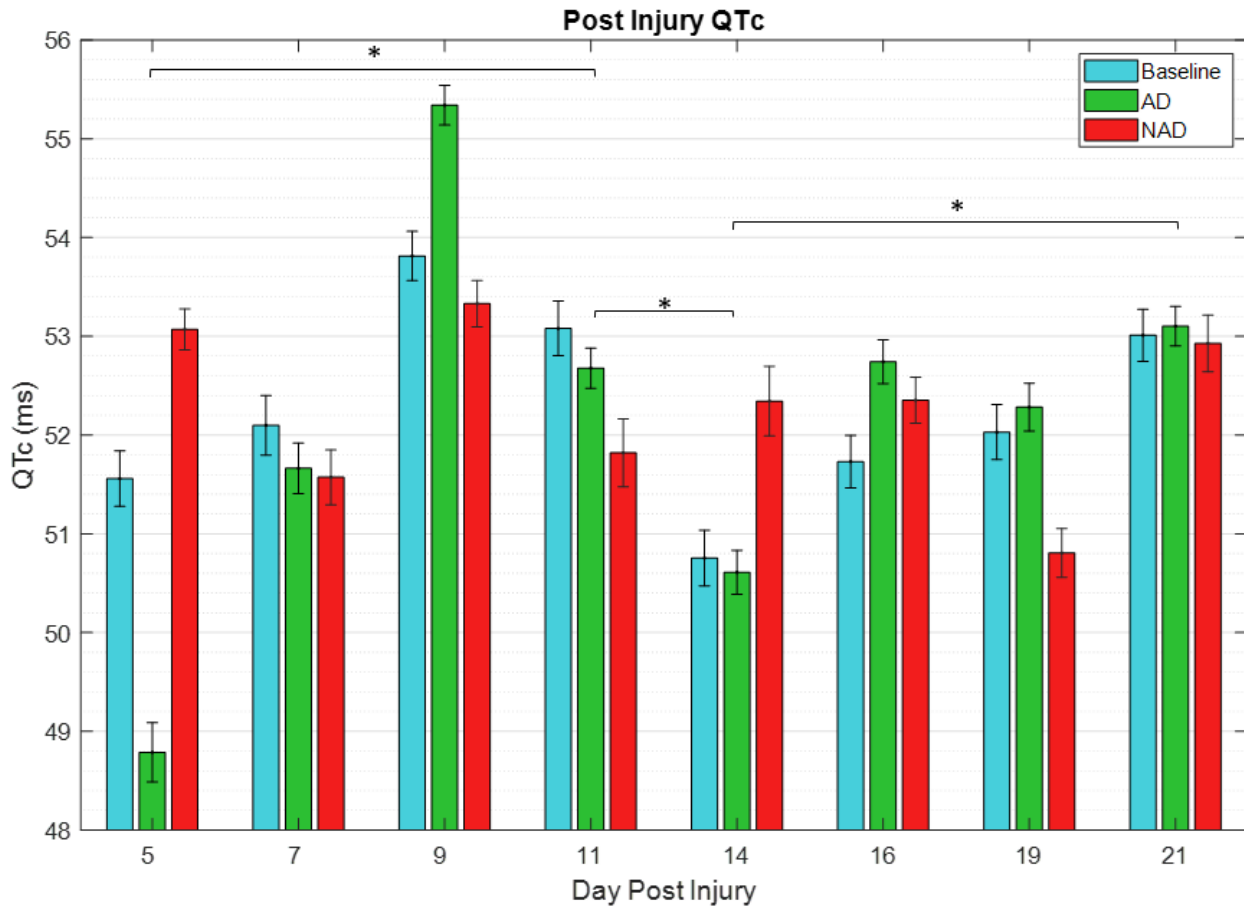


Figure 5.4. Change in QTc throughout experiment (* $p < 0.05$).

From the subacute to chronic phase (day 11 to day 14) there is a significant drop in QTc for both baseline ($53.08 \pm .28$ ms to $50.75 \pm .28$ ms) and AD events ($p < 0.05$). During NAD events there is a slight but insignificant increase.

During the chronic phase of SCI (day 14 to 21) there is a significant increase in baseline ($50.75 \pm .28$ ms to $53.01 \pm .26$ ms) and AD (50.61 ± 0.10 ms to 53.10 ± 0.09 ms) QTc ($p < 0.05$). During NAD the increase in QTc seen is not significant.

Over the subacute phase, baseline, AD, and NAD short term QTc variability (STVQTc) significantly decreased ($p < 0.05$). When there was no bursting activity the STVQTc significantly decreased from day 5 to day 11; however, during bursting activity there was a significant increase in STVQTc ($p < 0.05$) (Figure 5.5).

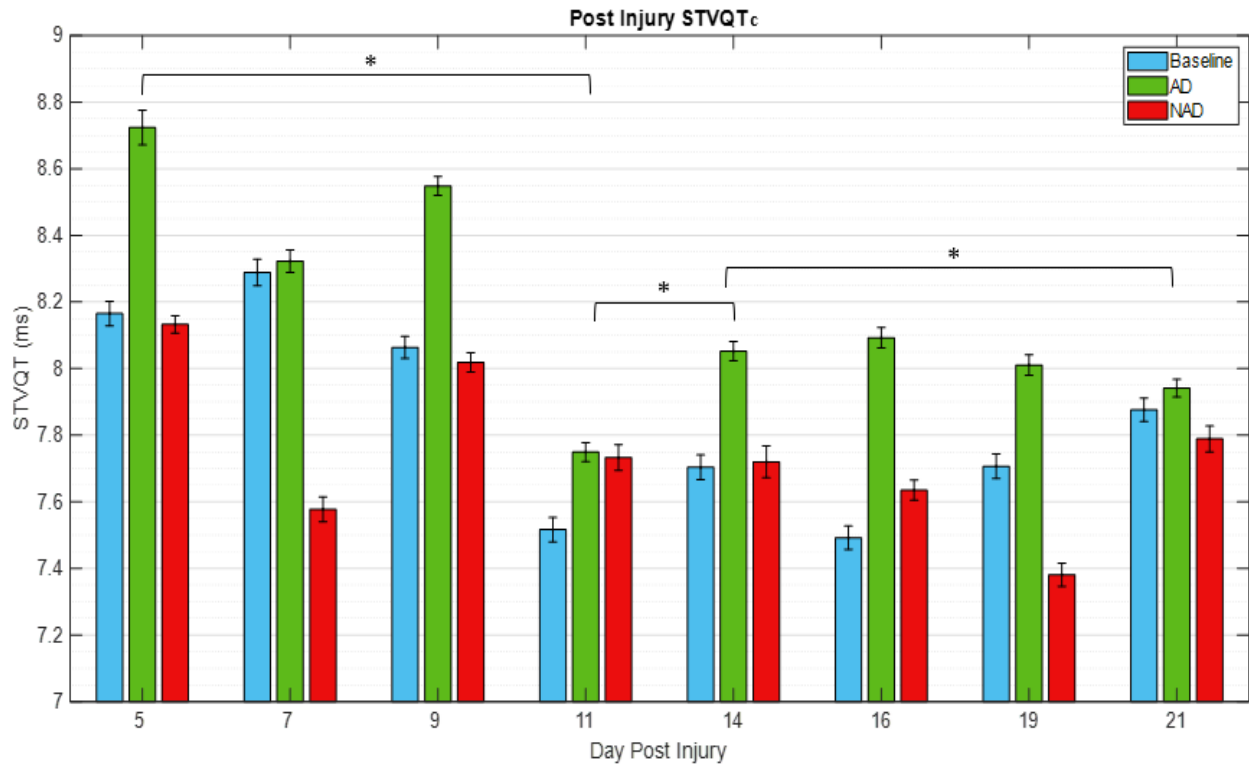


Figure 5.5. Change in STVQTc throughout experiment (* $p < 0.05$).

The STVQTc during AD events significantly decreased during the chronic phase, the NAD STVQTc increased; however, the increase is not deemed significant. During non-bursting there was also a significant decrease in STVQTc while an insignificant increase is seen during SKNA bursting activity.

Premature ventricular contractions (PVCs) are when the heartbeat is initiated by the Purkinje fibers instead of the sinoatrial node. Hypotension may result from a long run of PVCs (Khashayar & Richards, 2022). PVCs occurred a total of six times within three of the ten rats. Only three of which experienced PVCs. Two of these rats experienced only one PVC each, one of which occurred during an AD event on day five the other occurred during baseline on day 11. The third rat experienced four PVCs on day 19. On this day all three CRD trials resulted in AD, three of the PVCs occurred during CRD one and the other PVC was during CRD three. The third PVC of CRD one can be seen in Figure 5.6. The rat that experienced the most PVCs experienced 15 AD events during the CRD trials starting on day 7, which is two more than average. Nine of these AD events occurred between day 14 and 21. When the first PVC is documented the rat had

experienced 10 documented AD events with an additional two before the last PVC was documented.

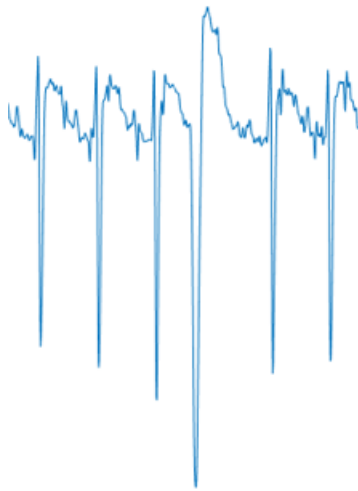


Figure 5.6. Example of a PVC.

For long term analysis of systolic blood pressure, heart rate, RR-interval, P-wave height, and QRS width a one-way ANOVA with a Tukey Kramer Post-hoc Test was run for each parameter. Throughout all trials the percent change from day 5 baseline systolic blood pressure, heart rate, and P-wave height and QRS similar trends to AD incidence. RR interval and QRS width followed an inverse pattern with relative peaks on day 14 instead of minimums. None of these parameters had a significant difference from day 14 to 21 (the chronic stage); however, heart rate, RR interval, and QRS width were significantly different from day 5 to day 11 (the subacute stage). There was also a significant decrease in RR interval from day 5 to day 21.

Overall systolic blood pressure significantly increased from 149.94 ± 0.15 mmHg to 155.54 ± 0.17 mmHg during the subacute phase ($p < 0.05$). It then significantly dropped to 152.17 ± 0.17 during the transition from subacute to chronic (day 11 to 14) ($p < 0.05$). During the chronic phase it increased from 152.17 ± 0.17 to 160.83 ± 0.17 ($p < 0.05$) (Figure 5.7). All three groups followed these same significant changes.

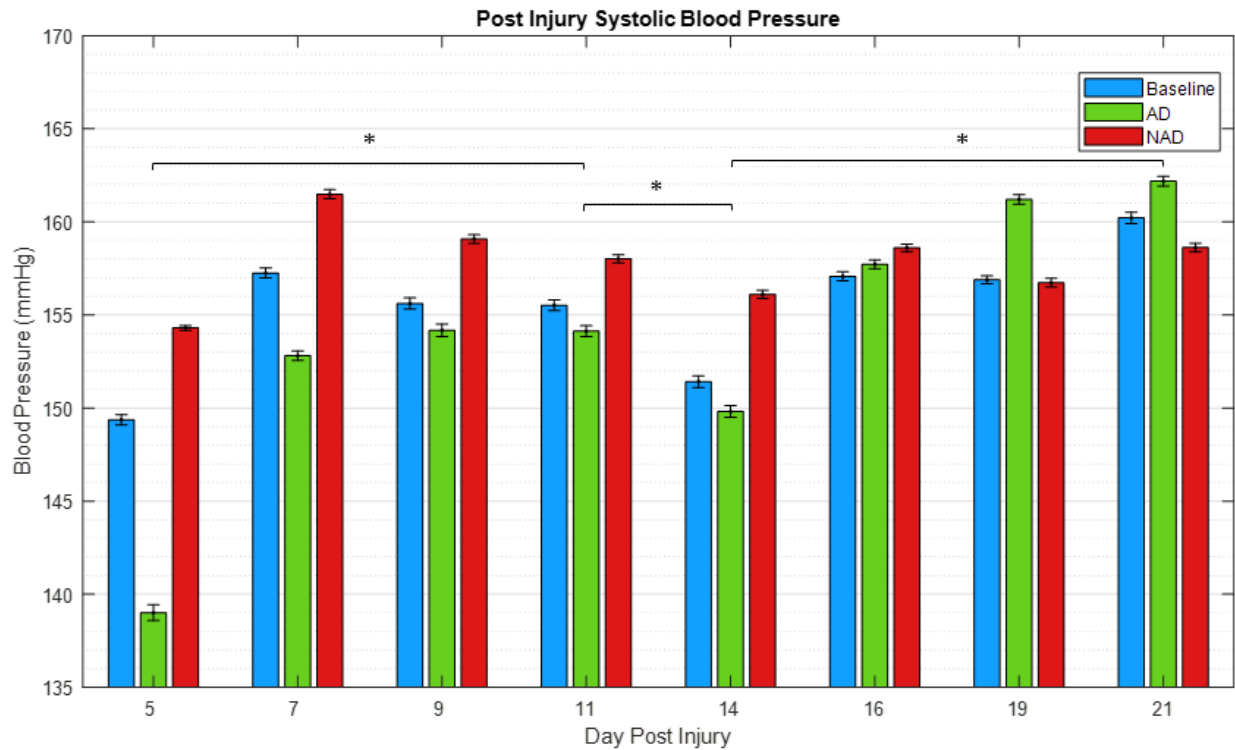


Figure 5.7. Change in systolic blood pressure post SCI (* $p < 0.05$).

The overall heart rate significantly increased during the subacute period (423.22 ± 0.62 to 479.97 ± 0.38 BPM) ($p < 0.05$). From the subacute to chronic phase heart rate dropped to 454.49 ± 0.48 BPM ($p < 0.05$). The chronic phase resulted in a significant increase to 466.50 ± 0.46 BPM ($p < 0.05$) (Figure 5.8). This overall significant increase is due to the NAD and baseline groups. The AD group saw a significant decrease during the chronic phase.

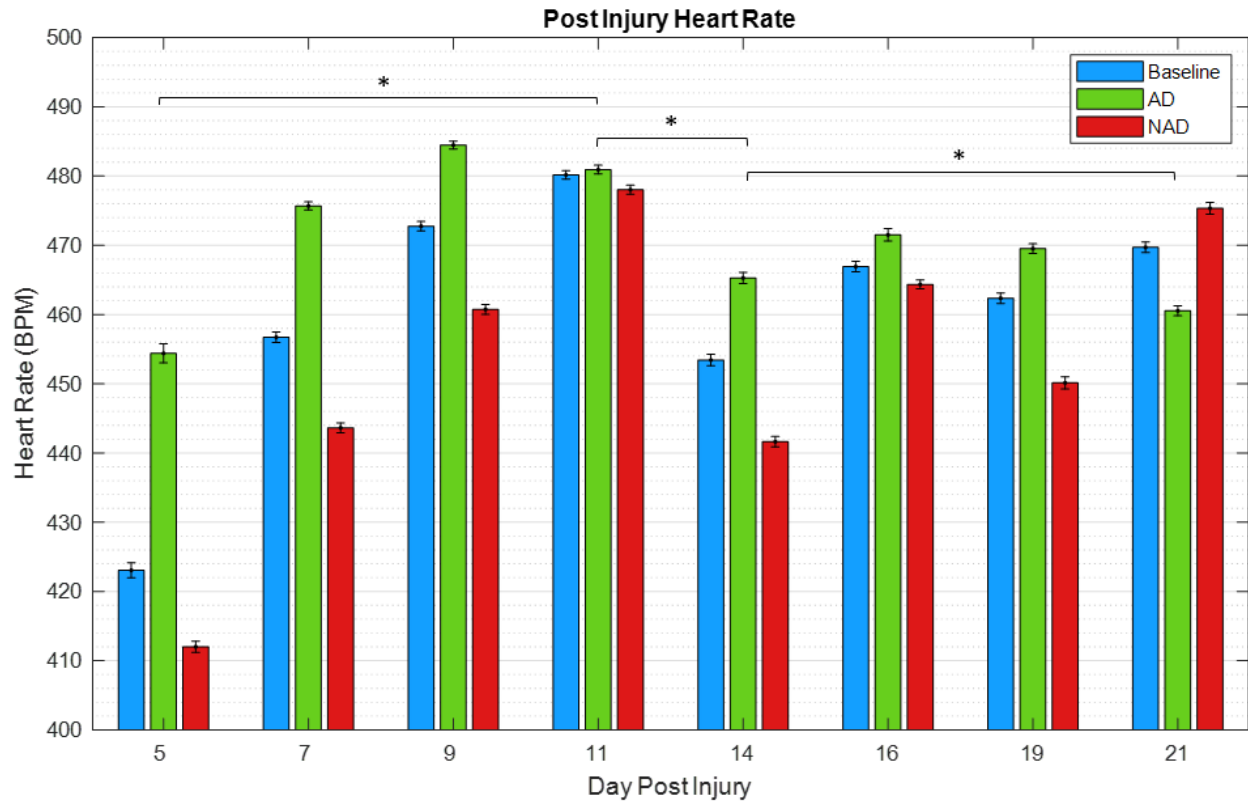


Figure 5.8. Change in heart rate post SCI (* $p < 0.05$).

During the days post SCI overall R-R interval had significant changes through the subacute phase, the transition from subacute to chronic, and during the chronic phase. It transitions from 146.12 ± 0.53 to 125.88 ± 0.19 ms during the subacute phase. Then during the chronic phase, R-R interval transitioned from 132.94 ± 0.15 to 129.63 ± 0.27 ms ($p < 0.05$) (Figure 5.9). Similarly to heart rate, AD did not follow the same trend as the other groups instead having a significant increase in RR interval during the chronic phase of SCI.

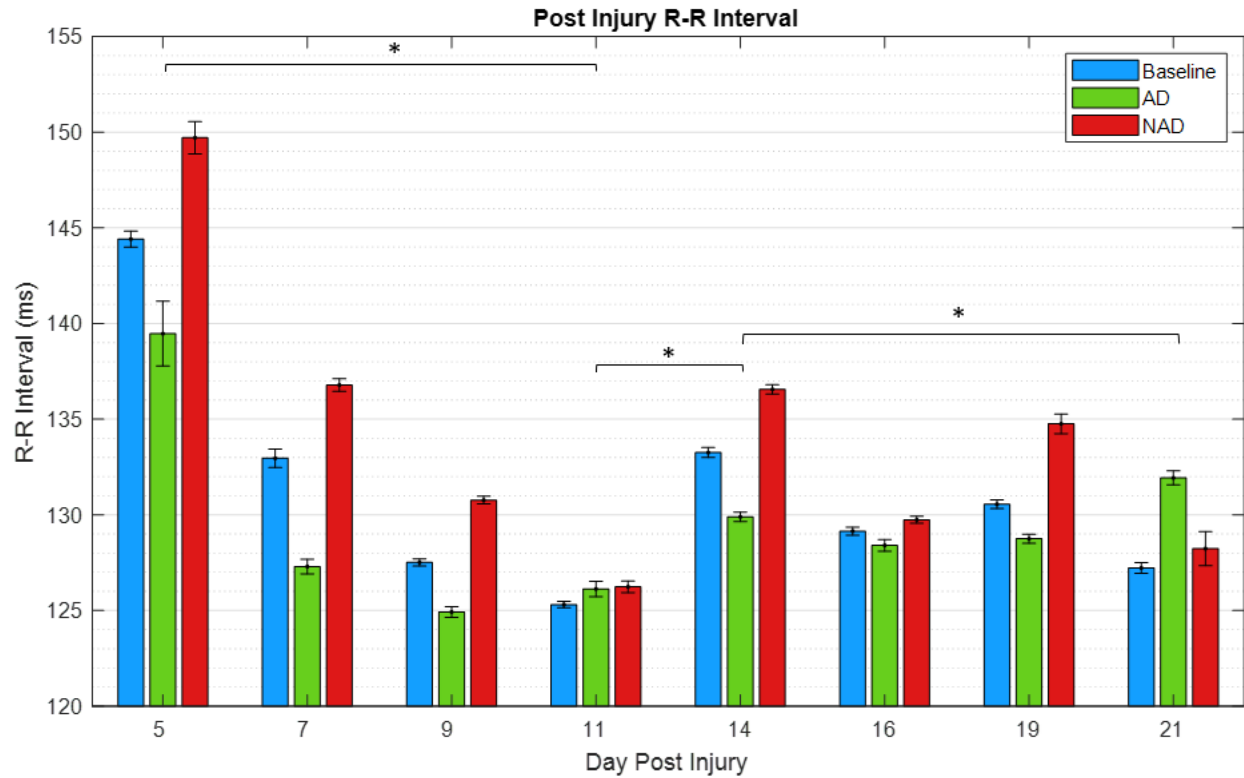


Figure 5.9. Change in R-R interval post SCI (* $p < 0.05$).

During the subacute period after SCI the overall P-wave height did not change significantly (day 5 vs. day 11). This is skewed by the baseline group. AD and NAD groups result in a significant decrease in P-wave height from day 5 to day 11. Overall, there was a significant difference between day 11 and 14 with a decrease of 0.0289 mV ($p < 0.05$). There was then a significant increase in P-wave height from day 14 to day 21, increasing from 0.1256 ± 0.0012 to 0.1413 ± 0.0009 mV ($p < 0.05$) (Figure 5.10). All three groups followed the same trend during the transition period and chronic stage of SCI.

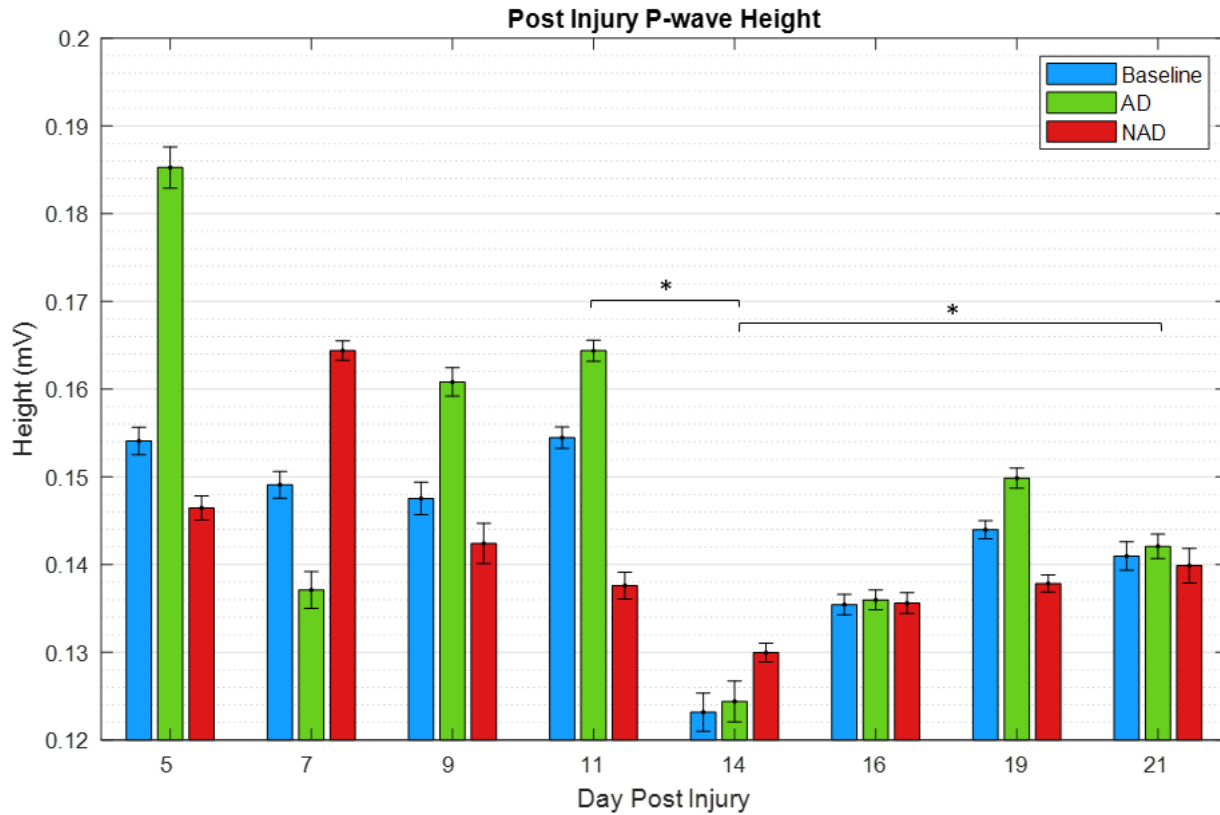


Figure 5.10. Change in P-wave height post SCI (* $p < 0.05$).

During the subacute phase overall QRS width decreased from 20.22 ± 0.02 to 18.91 ± 0.02 ms ($p < 0.05$). It also decreased during the chronic phase going from 19.35 ± 0.02 to 19.20 ± 0.02 ms ($p < 0.05$) (Figure 5.11). During the transition period of day 11 to day 14 all three groups had an increase in QRS width; however, the increase is not deemed significant for the NAD group. Many of the day-to-day comparisons of this parameter are not significant including day 16 vs 21 for the AD group and day 19 vs 21 for the baseline group.

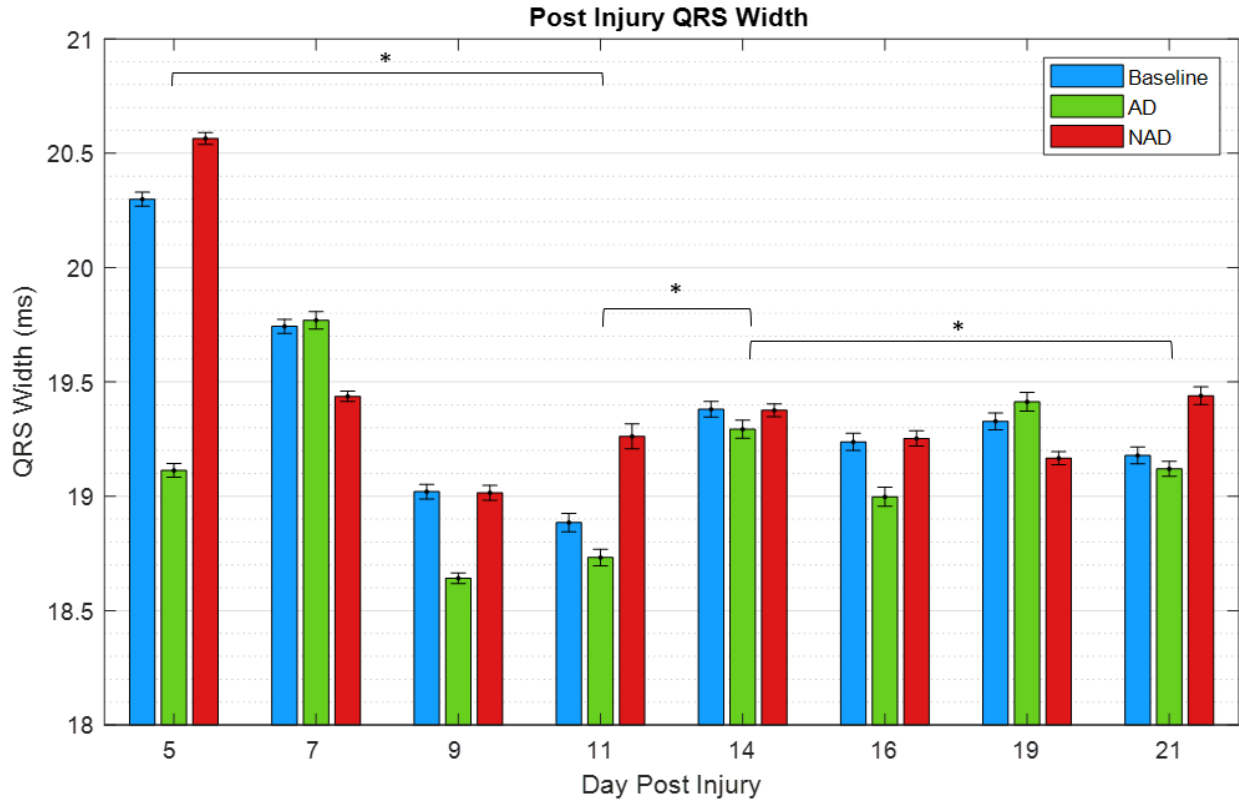


Figure 5.11. Change in QRS width post SCI (*p < 0.05).

5.3 Insights on Long-term Cardiac Effects

During the chronic phase the incidence of AD events increased during regular occurrences of CRD as indicated by above-threshold (≥ 15 mmHg) blood pressure spikes. QTc interval increased during the chronic phase resulting in potentially detrimental cardiac effects. This rat model showed that humans who experience recurrent AD during the chronic phase of SCI may be at increased risk for arrhythmia.

Throughout all long-term analysis parameters corresponded to the trend of AD incidence. However, not all these changes were significant throughout both the subacute and chronic stages. Often many of the day-to-day comparisons were not significant, but the difference between the beginning and end of the stage was.

There was a significant increase in P-wave height during the chronic stage of spinal cord injury. This increase suggests that recurrent AD may result in right atrial enlargement. The decrease in QRS width seen from day 14 to day 21 suggests that recurrent AD results in an increased risk of arrhythmia.

Frequent PVCs increase the risk of developing dilated cardiomyopathy. They also indicate an increased risk of mortality in individuals with heart disease (Khashayar & Richards, 2022). Heart disease is a leading cause of death in individuals with SCI an increased occurrence of PVCs could potentially increase the risk of death (Lee & Joo, 2017). As few PVCs were seen further study of PVC occurrence during recurring AD must be done for conclusive results.

6. CONCLUSIONS AND FUTURE DIRECTIONS

Corrected QT interval, short term variability of the QT interval, RR interval, P-wave height, and QRS width were analyzed during AD events and during both the subacute and chronic phases of AD. QT interval parameter and QRS width were investigated as changes mark an increased risk of arrhythmia, while P-wave height shows atrial health, and RR interval is representative of heart rate. For this a rat model of a T2/T3 crush spinal cord injury was used. Colorectal distension was implemented to induce AD events a total of 24 times for each rat. Ponemah® was used to extract heart rate, blood pressure, RR interval, P-wave height, and QRS width values. MATLAB code was implemented to find the QT interval.

It was found that during AD events there is a significant increase in QTc, STVQTc, average systolic blood pressure, and P-wave height. It was also seen that there was a significant decrease in QRS width during AD events. These results suggest that there is an increased risk of arrhythmia during AD events. The hypothesis that QT interval variability would increase during an AD event failed to be rejected while the hypothesis that RR interval, P-wave height and QRS width would increase during an AD event was rejected. P-wave height did in fact increase, however QRS width decreased, and there was no significant change in RR interval.

Long term analysis showed that during the chronic phase of SCI P-wave height, QTc interval, and STVQTc all increased during baseline recordings while QRS width decreased. AD events also showed a significant increase in QTc and P-wave height with a significant decrease in QRS width during the chronic stage. These results show that recurrent AD may increase the risk of arrhythmia during both baseline and AD events and increases the strain on the atria potentially causing right atrial enlargement. With these results the hypothesis that AD occurrence would result in decreased heart function and increased risk of arrhythmias failed to be rejected.

6.1 Conclusions

This exploratory research was based on two case reports published in 1991 stating that AD can result in arrhythmia (Pine et al.,1991; Forrest, 1991). Arrhythmias can result in sudden cardiac death, so it is important to know how AD effects the occurrence of arrhythmia so proper medical intervention is in place (Srinivasan & Schilling, 2018).

Knowing that recurrent AD may increase the risk of arrhythmia during AD events themselves and during baseline in the chronic stage of spinal cord injury, individuals who are susceptible to AD should be monitored for arrhythmias. Individuals who are being monitored for AD could use the same device to monitor changes in their ECG, specifically changes to the QTc interval, QTc variability, and QRS width. Trends in the changes of these parameters could be used by healthcare providers to monitor arrhythmia risk and implement preventative measures when necessary.

6.2 Limitations and Possible Modifications

In this study the occurrence of AD in each animal varied significantly limiting day to day analysis as no rat had the same pattern of AD events. While Sprague Dawley rats are commonly used in SCI research Wistar rats are also common models. The advantage of Wistar rats is that they are more prone to AD through CRD (Landrum et al., 1998). Wistar rats would potentially result in more consistent AD occurrences allowing for a better analysis of parameter changes due to AD. A sham control group would also be beneficial as SCI itself causes cardiac functionality changes. A sham group would allow for a better analysis of if recurrent AD results in changes past that of SCI.

While SCI surgeries, animal care, and experiment protocols were consistent throughout, interactions were not kept at a consistent time of day and were subject to class schedules. This may have added variability to the results as QT interval varies throughout the day due to circadian rhythm and other factors (Smetana et al., 2003). Spontaneous AD may have also affected results as the rats were not monitored 24/7. Some days of data collection had to be removed from analysis due to noise in the signal reducing the total data set. In the future a Faraday cage to block external uncontrolled influences of the signal should be used.

The duration of experimentation also limited the results; however, maintaining health of the animal to 21 days post injury was difficult. Some studies don't consider the chronic stage of SCI in a rodent model to fully begin until week eight post injury (Martín-López et al., 2021). A longer study would be beneficial for understanding long term changes.

6.3 Future Directions

In the future the same general experiment could be performed using some of the suggestions above including changing rat type, introducing a Faraday cage, remaining consistent in timing for all experiment days and extending the post-op analysis time to at least eight weeks. Further analysis of current data could include P-T segment and analyzing how burst SKNA activity effects parameters other than QTc such as QRS width. In addition to see the true effects of arrhythmia risk in the future predisposing the rats to arrhythmia through chemical intervention could be used (Fernandes et al., 2022).

An understanding of how these results transfer to a human model would also be necessary to understand how recurrent AD affects the cardiovascular system. Humans are more susceptible to arrhythmias than rodent models (Blackwell et al., 1964; Hasenfuss, 1998).

REFERENCES

- A. A. R. Bsoul, S. -Y. Ji, K. Ward, and K. Najarian, "Detection of P, QRS, and T Components of ECG using wavelet transformation," 2009 ICME International Conference on Complex Medical Engineering, Tempe, AZ, USA, 2009, pp. 1-6, doi: 10.1109/ICCME.2009.4906677.
- AD Instruments. (n.d.). *Guide to DSI's implantable - adinstruments*. DSI-Implantable-Telemetry-Devices.<http://m-cdn.adinstruments.com/brochures/DSI-Implantable-Telemetry-Devices.pdf>
- Ahuja, C., Wilson, J., Nori, S. et al. Traumatic spinal cord injury. *Nat Rev Dis Primers* 3, 17018 (2017). <https://doi.org/10.1038/nrdp.2017.18>
- Akhtar, A. Z., Pippin, J. J., & Sandusky, C. B. (2009). Animal Studies in spinal cord injury: A systematic review of Methylprednisolone. *Alternatives to Laboratory Animals*, 37(1), 43–62. <https://doi.org/10.1177/026119290903700108>
- Al-Akchar, M., & Siddique, MS. (2022, December). *Long QT Syndrome*. StatPearls [Internet]. <https://www.ncbi.nlm.nih.gov/books/NBK441860/>
- Allen, K., & Leslie, S. (2023, January). *Autonomic Dysreflexia*. StatPearls [Internet] . <https://www.ncbi.nlm.nih.gov/books/NBK482434/>
- Alshak, M. N., & Das, J. M. (2023, May). *Neuroanatomy, Sympathetic Nervous System*. StatPearls [Internet]. <https://www.ncbi.nlm.nih.gov/books/NBK542195/>
- Ambhore, A., Teo, S. G., Bin Omar, A. R., & Poh, K. K. (2014). Importance of QT interval in clinical practice. *Singapore medical journal*, 55(12), 607–612. <https://doi.org/10.11622/smedj.2014172>
- Armstrong, M., Kerndt, C., & Moore, R. (2023, March). *Physiology, Baroreceptors* . StatPearls [Internet]. <https://www.ncbi.nlm.nih.gov/books/NBK538172/>
- Ashley, E., & Niebauer, J. (2004). *Conquering the ECG - cardiology explained - NCBI bookshelf*. NIH. <https://www.ncbi.nlm.nih.gov/books/NBK2214/>
- Badr, M., Al-Otaibi, S., Alturki, N., & Abir, T. (2022). Detection of Heart Arrhythmia on Electrocardiogram using Artificial Neural Networks. *Computational intelligence and neuroscience*, 2022, 1094830. <https://doi.org/10.1155/2022/1094830>
- Banek, C. T., Bradshaw, J. L., Coats, L. E., Alexander, B. T., & Goulopoulou, S. (2021). Getting it right: Preventing drift in baseline cardiovascular phenotype when using Sprague–Dawley rats. *American Journal of Physiology-Heart and Circulatory Physiology*, 321(3). <https://doi.org/10.1152/ajpheart.00382.2021>

- Baumert, M., Porta, A., Vos, M. A., Malik, M., Couderc, J. P., Laguna, P., Piccirillo, G., Smith, G. L., Tereshchenko, L. G., & Volders, P. G. (2016). QT interval variability in body surface ECG: measurement, physiological basis, and clinical value: position statement and consensus guidance endorsed by the European Heart Rhythm Association jointly with the ESC Working Group on Cardiac Cellular Electrophysiology. *Europace : European pacing, arrhythmias, and cardiac electrophysiology : journal of the working groups on cardiac pacing, arrhythmias, and cardiac cellular electrophysiology of the European Society of Cardiology*, 18(6), 925–944. <https://doi.org/10.1093/europace/euv405>
- Baumert, M., Schlaich, M. P., Nalivaiko, E., Lambert, E., Sari, C. I., Kaye, D. M., Elser, M. D., Sanders, P., & Lambert, G. (2011). Relation between QT interval variability and cardiac sympathetic activity in hypertension. *American Journal of Physiology-Heart and Circulatory Physiology*, 300(4). <https://doi.org/10.1152/ajpheart.01184.2010>
- Bigger, J. T. (1983). Definition of benign versus malignant ventricular arrhythmias: Targets for treatment. *The American Journal of Cardiology*, 52(6). [https://doi.org/10.1016/0002-9149\(83\)90632-x](https://doi.org/10.1016/0002-9149(83)90632-x)
- Blackwell, D. J., Schmeckpeper, J., & Knollmann, B. C. (2022). Animal models to study cardiac arrhythmias. *Circulation Research*, 130(12), 1926–1964. <https://doi.org/10.1161/circresaha.122.320258>
- Brower, M., Grace, M., Kotz, C. M., & Koya, V. (2015). Comparative analysis of growth characteristics of Sprague Dawley rats obtained from different sources. *Laboratory animal research*, 31(4), 166–173. <https://doi.org/10.5625/lar.2015.31.4.166>
- Cesarovic, N., Jirkof, P., Rettich, A., & Arras, M. (2011). Implantation of radiotelemetry transmitters yielding data on ECG, heart rate, core body temperature and activity in free-moving laboratory mice. *Journal of visualized experiments : JoVE*, (57), 3260. <https://doi.org/10.3791/3260>
- Charkoudian, N., & Rabbitts, J. A. (2009). Sympathetic neural mechanisms in human cardiovascular health and disease. *Mayo Clinic proceedings*, 84(9), 822–830. [https://doi.org/10.1016/S0025-6196\(11\)60492-8](https://doi.org/10.1016/S0025-6196(11)60492-8)
- Chen, J.-J., Lin, C., Hsiao, W., Chu, T.-M., Yang, H.-W., Lo, M.-T., Lin, L.-Y., & Lin, S.-F. (2021). Complex dynamics of skin sympathetic nerve activities as a prognostic predictor for critically ill patients. *Journal of the Formosan Medical Association*, 120(1), 660–667. <https://doi.org/10.1016/j.jfma.2020.07.025>
- Chen, S., Meng, G., Doytchinova, A., Wong, J., Straka, S., Lacy, J., Li, X., Chen, P.-S., & Everett IV, T. H. (2021). Skin sympathetic nerve activity and the short-term QT interval variability in patients with electrical storm. *Frontiers in Physiology*, 12. <https://doi.org/10.3389/fphys.2021.742844>

- Chung, F.-P., Hu, Y.-F., Chao, T.-F., Higa, S., Cheng, H., Lin, Y.-J., Chang, S.-L., Lo, L.-W., Tuan, T.-C., Tai, C.-T., Li, C.-H., Lin, Y.-K., & Chen, S.-A. (2011). The correlation between ventricular repolarization and clinical severity of spinal cord injuries. *Heart Rhythm*, 8(6), 879–884. <https://doi.org/10.1016/j.hrthm.2011.01.034>
- Cloutier, S., LaFollette, M. R., Gaskill, B. N., Panksepp, J., & Newberry, R. C. (2018). Tickling, a Technique for Inducing Positive Affect When Handling Rats. *Journal of visualized experiments : JoVE*, (135), 57190. <https://doi.org/10.3791/57190>
- Cloutier, S., LaFollette, M. R., Gaskill, B. N., Panksepp, J., & Newberry, R. C. (2018). Tickling, a Technique for Inducing Positive Affect When Handling Rats. *Journal of visualized experiments : JoVE*, (135), 57190. <https://doi.org/10.3791/57190>
- Cole, S., Donoghue, T., Gao, R., & Voytek, B. (2019). NeuroDSP: A package for neural digital signal processing. *Journal of Open Source Software*, 4(36), 1272. <https://doi.org/10.21105/joss.01272>
- Cragg, J., & Krassioukov, A. (2012). Autonomic dysreflexia. *CMAJ : Canadian Medical Association journal = journal de l'Association medicale canadienne*, 184(1), 66. <https://doi.org/10.1503/cmaj.110859>
- Diedrich, A., Jordan, J., Shannon, J. R., Robertson, D., & Biaggioni, I. (2002). Modulation of QT interval during autonomic nervous system blockade in humans. *Circulation*, 106(17), 2238–2243. <https://doi.org/10.1161/01.cir.0000035241.76918.6c>
- Douedi, S., & Douedi, H. (2022, July). *P wave*. StatPearls [Internet]. <https://www.ncbi.nlm.nih.gov/books/NBK551635/>
- Doytchinova, A., Hassel, J. L., Yuan, Y., Lin, H., Yin, D., Adams, D., Straka, S., Wright, K., Smith, K., Wagner, D., Shen, C., Salanova, V., Meshberger, C., Chen, L. S., Kincaid, J. C., Coffey, A. C., Wu, G., Li, Y., Kovacs, R. J., ... Chen, P.-S. (2017). Simultaneous noninvasive recording of skin sympathetic nerve activity and electrocardiogram. *Heart Rhythm*, 14(1), 25–33. <https://doi.org/10.1016/j.hrthm.2016.09.019>
- Everett, T. H., 4th, Doytchinova, A., Cha, Y. M., & Chen, P. S. (2017). Recording sympathetic nerve activity from the skin. *Trends in cardiovascular medicine*, 27(7), 463–472. <https://doi.org/10.1016/j.tcm.2017.05.003>
- Fernandes, S., Oatman, E., Weinberger, J., Dixon, A., Osei-Owusu, P., & Hou, S. (2022). The susceptibility of cardiac arrhythmias after spinal cord crush injury in rats. *Experimental neurology*, 357, 114200. <https://doi.org/10.1016/j.expneurol.2022.114200>
- Forrest G. P. (1991). Atrial fibrillation associated with autonomic dysreflexia in patients with tetraplegia. *Archives of physical medicine and rehabilitation*, 72(8), 592–594.

- Fossey, M. P. M., Balthazaar, S. J. T., Squair, J. W., Williams, A. M., Poormasjedi-Meibod, M. S., Nightingale, T. E., Erskine, E., Hayes, B., Ahmadian, M., Jackson, G. S., Hunter, D. V., Currie, K. D., Tsang, T. S. M., Walter, M., Little, J. P., Ramer, M. S., Krassioukov, A. V., & West, C. R. (2022). Spinal cord injury impairs cardiac function due to impaired bulbospinal sympathetic control. *Nature communications*, 13(1), 1382. <https://doi.org/10.1038/s41467-022-29066-1>
- Furusawa, K., Tokuhiro, A., Sugiyama, H. et al. Incidence of symptomatic autonomic dysreflexia varies according to the bowel and bladder management techniques in patients with spinal cord injury. *Spinal Cord* 49, 49–54 (2011). <https://doi.org/10.1038/sc.2010.94>
- Gordan, R., Gwathmey, J. K., & Xie, L. H. (2015). Autonomic and endocrine control of cardiovascular function. *World journal of cardiology*, 7(4), 204–214. <https://doi.org/10.4330/wjc.v7.i4.204>
- Grigorean, V. T., Sandu, A. M., Popescu, M., Iacobini, M. A., Stoian, R., Neascu, C., Strambu, V., & Popa, F. (2009). Cardiac dysfunctions following spinal cord injury. *Journal of medicine and life*, 2(2), 133–145.
- Hall, J. E. (2021). Functional Organization of the Human Body and Control of the “Internal Environment.” In *Guyton and Hall Textbook of Medical Physiology* (12th ed., pp. 3–9). essay, Elsevier.
- Harvey, L. (2008). Background information. In *Management of spinal cord injuries a guide for physiotherapists* (pp. 3–33). essay, Churchill Livingstone/Elsevier. Retrieved July 12, 2023, from https://www.sciencedirect.com/science/article/pii/B9780443068584500071?ref=pdf_download&fr=RR-2&rr=7e5cfde52ea0ef6f.
- Hasenfuss, G. (1998). Animal models of human cardiovascular disease, heart failure and hypertrophy. *Cardiovascular Research*, 39(1), 60–76. [https://doi.org/10.1016/s0008-6363\(98\)00110-2](https://doi.org/10.1016/s0008-6363(98)00110-2)
- HD-S Device Surgical Manual. (n.d.).
- Heffernan, K. S., Jae, S. Y., Lee, M., Mojtahedi, M., Evans, E. M., Zhu, W., & Fernhall, B. (2007). Gender differences in QTC interval in young, trained individuals with lower spinal cord injury. *Spinal Cord*, 45(7), 518–521. <https://doi.org/10.1038/sj.sc.3102049>
- Henke, A. M., Billington, Z. J., & Gater, D. R., Jr (2022). Autonomic Dysfunction and Management after Spinal Cord Injury: A Narrative Review. *Journal of personalized medicine*, 12(7), 1110. <https://doi.org/10.3390/jpm12071110>
- Hou, S., Blesch, A., & Lu, P. (2014). A radio-telemetric system to monitor cardiovascular function in rats with spinal cord transection and embryonic neural stem cell grafts. *Journal of Visualized Experiments*, (92). <https://doi.org/10.3791/51914>

- Isoda, W. C., & Segal, J. L. (2003). Effects of 4-aminopyridine on cardiac repolarization, PR interval, and heart rate in patients with spinal cord injury. *Pharmacotherapy*, 23(2), 133–136. <https://doi.org/10.1592/phco.23.2.133.32089>
- Jaffe, T., & Thompson, W. M. (2015). Large-bowel obstruction in the adult: Classic radiographic and CT findings, etiology, and mimics. *Radiology*, 275(3), 651–663. <https://doi.org/10.1148/radiol.2015140916>
- Khashayar, F., & Richards, J. (2022, December). *Premature Ventricular Contraction*. StatPearls [Internet]. <https://www.ncbi.nlm.nih.gov/books/NBK532991/>
- Kirby, A. K. (2022). *TIME AND FREQUENCY DOMAIN ANALYSIS OF PHYSIOLOGICAL FEATURES DURING AUTONOMIC DYSREFLEXIA AFTER SPINAL CORD INJURY* (thesis).
- Kirby, A. Pancholi, S., Suresh, S., Anderson, Z., Chesler, C., Everett, IV, T.H., Duerstock, B.S. Acclimation Protocol to Minimize Stress in Immobilized Rats During Non-Invasive Multimodal Sensing of the Autonomic Nervous System. *Military Medicine*, Warfighters supplement, In press.
- Kjell, J., & Olson, L. (2016). Rat models of spinal cord injury: from pathology to potential therapies. *Disease models & mechanisms*, 9(10), 1125–1137. <https://doi.org/10.1242/dmm.025833>
- Kmecova, J., & Klimas, J. (2010). Heart rate correction of the QT duration in rats. *European journal of pharmacology*, 641(2-3), 187–192. <https://doi.org/10.1016/j.ejphar.2010.05.038>
- Krassioukov, A. V., & Weaver, L. C. (1995). Episodic hypertension due to autonomic dysreflexia in acute and chronic spinal cord-injured rats. *American Journal of Physiology-Heart and Circulatory Physiology*, 268(5). <https://doi.org/10.1152/ajpheart.1995.268.5.h2077>
- La Rovere, M. T., & Christensen, J. H. (2015). The autonomic nervous system and cardiovascular disease: Role of N-3 pufas. *Vascular Pharmacology*, 71, 1–10. <https://doi.org/10.1016/j.vph.2015.02.005>
- Landrum, L. M., Thompson, G. M., & Blair, R. W. (1998). Does postsynaptic α 1-adrenergic receptor supersensitivity contribute to autonomic dysreflexia? *American Journal of Physiology-Heart and Circulatory Physiology*, 274(4). <https://doi.org/10.1152/ajpheart.1998.274.4.h1090>
- Lee, E. S., & Joo, M. C. (2017). Prevalence of Autonomic Dysreflexia in Patients with Spinal Cord Injury above T6. *BioMed research international*, 2017, 2027594. <https://doi.org/10.1155/2017/2027594>

- Linsenmeyer, T.A., Gibbs, K. & Solinsky, R. Autonomic Dysreflexia After Spinal Cord Injury: Beyond the Basics. *Curr Phys Med Rehabil Rep* 8, 443–451 (2020). <https://doi.org/10.1007/s40141-020-00300-5>
- Martín-López, M., González-Muñoz, E., Gómez-González, E., Sánchez-Pernaute, R., Márquez-Rivas, J., & Fernández-Muñoz, B. (2021). Modeling chronic cervical spinal cord injury in aged rats for cell therapy studies. *Journal of Clinical Neuroscience*, 94, 76–85. <https://doi.org/10.1016/j.jocn.2021.09.042>
- McCorry L. K. (2007). Physiology of the autonomic nervous system. *American journal of pharmaceutical education*, 71(4), 78. <https://doi.org/10.5688/aj710478>
- Mestre, H., Ramirez, M., Garcia, E., Martinon, S., Cruz, Y., Campos, M. G., & Ibarra, A. (2015). Lewis, fischer 344, and Sprague-Dawley rats display differences in lipid peroxidation, motor recovery, and Rubrospinal Tract Preservation after Spinal Cord Injury. *Frontiers in Neurology*, 6. <https://doi.org/10.3389/fneur.2015.00108>
- National Spinal Cord Injury Statistical Center, Traumatic Spinal Cord Injury Facts and Figures at a Glance. Birmingham, AL: University of Alabama at Birmingham, 2023
- Ness, T. J., & Gebhart, G. F. (1988). Colorectal distension as a noxious visceral stimulus: Physiologic and pharmacologic characterization of pseudoaffective reflexes in the rat. *Brain Research*, 450(1–2), 153–169. [https://doi.org/10.1016/0006-8993\(88\)91555-7](https://doi.org/10.1016/0006-8993(88)91555-7)
- O'Mahony, S. M., Tramullas, M., Fitzgerald, P., & Cryan, J. F. (2012). Rodent models of colorectal distension. *Current protocols in neuroscience*, Chapter 9, . <https://doi.org/10.1002/0471142301.ns0940s61>
- Patel, T. R. (2015). Anatomy of the sympathetic nervous system. *Nerves and Nerve Injuries*, 1, 495–506. <https://doi.org/10.1016/b978-0-12-410390-0.00038-x>
- Pine, Z. M., Miller, S. D., & Alonso, J. A. (1991). Atrial fibrillation associated with autonomic dysreflexia. *American journal of physical medicine & rehabilitation*, 70(5), 271–273. <https://doi.org/10.1097/00002060-199110000-00008>
- Ramsey, J. B. G., Ramer, L. M., Inskip, J. A., Alan, N., Ramer, M. S., & Krassioukov, A. v. (2010). Care of Rats with Complete High-Thoracic Spinal Cord Injury. *Journal of Neurotrauma*, 27(9), 1709–1722.
- S. Hargittai, "Savitzky-Golay least-squares polynomial filters in ECG signal processing," *Computers in Cardiology*, 2005, Lyon, France, 2005, pp. 763-766, doi: 10.1109/CIC.2005.1588216.
- Sharif, H., & Hou, S. (2017). Autonomic dysreflexia: a cardiovascular disorder following spinal cord injury. *Neural regeneration research*, 12(9), 1390–1400. <https://doi.org/10.4103/1673-5374.215241>

- Sharif-Alhoseini, M., Khormali, M., Rezaei, M. et al. Animal models of spinal cord injury: a systematic review. *Spinal Cord* 55, 714–721 (2017). <https://doi.org/10.1038/sc.2016.187>
- Smetana, P., Batchvarov, V., Hnatkova, K., Camm, A. J., & Malik, M. (2003). Circadian rhythm of the corrected QT interval: impact of different heart rate correction models. *Pacing and clinical electrophysiology : PACE*, 26(1P2), 383–386. <https://doi.org/10.1046/j.1460-9592.2003.00054.x>
- Smoczyńska, A., Loen, V., Sprenkeler, D. J., Tuinenburg, A. E., Ritsema van Eck, H. J., Malik, M., Schmidt, G., Meine, M., & Vos, M. A. (2020). Short-term variability of the QT interval can be used for the prediction of imminent ventricular arrhythmias in patients with primary prophylactic implantable cardioverter defibrillators. *Journal of the American Heart Association*, 9(23). <https://doi.org/10.1161/jaha.120.018133>
- Squair, J. W., West, C. R., Popok, D., Assinck, P., Liu, J., Tetzlaff, W., & Krassioukov, A. v. (2017). High thoracic contusion model for the investigation of cardiovascular function after spinal cord injury. *Journal of Neurotrauma*, 34(3), 671–684. <https://doi.org/10.1089/neu.2016.4518>
- Srinivasan, N. T., & Schilling, R. J. (2018). Sudden Cardiac Death and Arrhythmias. *Arrhythmia & electrophysiology review*, 7(2), 111–117. <https://doi.org/10.15420/aer.2018:15:2>
- Suresh, S. and Duerstock, B.S. (2020) Automated Detection of Symptomatic Autonomic Dysreflexia through Multimodal Sensing. *IEEE Journal of Translational Engineering in Health and Medicine*, 8, 1-8. DOI: 10.1109/JTEHM.2019.2955947
- Suresh, S., Everett, T. H., 4th, Shi, R., & Duerstock, B. S. (2022). Automatic Detection and Characterization of Autonomic Dysreflexia Using Multi-Modal Non-Invasive Sensing and Neural Networks. *Neurotrauma reports*, 3(1), 501–510. <https://doi.org/10.1089/neur.2022.0041>
- Tindle, J., & Tadi, P. (2022, October 31). *Neuroanatomy, Parasympathetic Nervous System*. <https://www.ncbi.nlm.nih.gov/books/NBK553141/>. <https://www.ncbi.nlm.nih.gov/books/NBK553141/>
- Tiwari, A. kumar. (2021). *Automatic Detection of Q-T Interval in ECG Using MATLAB Tool*. <https://doi.org/10.21203/rs.3.rs-970625/v1>
- U.S. Department of Health and Human Services. (2022, August). *Why animals are used in research*. National Institutes of Health. <https://grants.nih.gov/grants/policy/air/why.htm#:~:text=Animal%20studies%20conducted%20in%20the,light%2C%20diet%2C%20or%20medications.>
- U.S. Department of Health and Human Services. (2023a, January 20). *Orthostatic Hypotension*. National Institute of Neurological Disorders and Stroke. <https://www.ninds.nih.gov/health-information/disorders/orthostatic-hypotension#:~:text=Orthostatic%20hypotension%20is%20a%20condition,or%20lightheadedness%20when%20standing%20up>

- U.S. Department of Health and Human Services. (2023b, January 20). *Spinal Cord Injury*. National Institute of Neurological Disorders and Stroke. <https://www.ninds.nih.gov/health-information/disorders/spinal-cord-injury>
- van den Berg, M. E., Kors, J. A., van Herpen, G., Bots, M. L., Hillege, H., Swenne, C. A., Stricker, B. H., & Rijnbeek, P. R. (2019). Normal values of qt variability in 10-S electrocardiograms for all ages. *Frontiers in Physiology*, 10. <https://doi.org/10.3389/fphys.2019.01272>
- Vázquez-Seisdedos, C.R., Neto, J.E., Marañón Reyes, E.J. et al. New approach for T-wave end detection on electrocardiogram: Performance in noisy conditions. *BioMed Eng OnLine* 10, 77 (2011). <https://doi.org/10.1186/1475-925X-10-77>
- Wang, C.-C., Chang, C.-T., Lin, C.-L., Huang, B.-R., & Kao, C.-H. (2016). Spinal cord injury is associated with an increased risk of atrial fibrillation: A population-based Cohort Study. *Heart Rhythm*, 13(2), 416–423. <https://doi.org/10.1016/j.hrthm.2015.10.021>
- Waxenbaum, J., Reddy, V., & Varacallo, M. (2022, July). *Anatomy, Autonomic Nervous System*. StatPearls [Internet]. <https://www.ncbi.nlm.nih.gov/books/NBK539845/>
- Wecht, J. M., Harel, N. Y., Guest, J., Kirshblum, S. C., Forrest, G. F., Bloom, O., Ovechkin, A. V., & Harkema, S. (2020). Cardiovascular Autonomic Dysfunction in Spinal Cord Injury: Epidemiology, Diagnosis, and Management. *Seminars in neurology*, 40(5), 550–559. <https://doi.org/10.1055/s-0040-1713885>
- Wolpert, C., Veltmann, C., Schimpf, R., Antzelevitch, C., Gussak, I., & Borggrefe, M. (2008). Is a narrow and tall QRS complex an ECG marker for sudden death?. *Heart rhythm*, 5(9), 1339–1345. <https://doi.org/10.1016/j.hrthm.2008.05.019>
- World Health Organization. (2013, November 19). *Spinal Cord Injury*. World Health Organization. <https://www.who.int/news-room/fact-sheets/detail/spinal-cord-injury#:~:text=Spinal%20cord%20injury%20is%20associated%20with%20a%20risk%20of%20developing,chronic%20pain%2C%20and%20respiratory%20complications>

PUBLICATIONS

- Anderson, Z., Dye, M., Sanchez, M., Duerstock, B.S., Everett, T.H. IV “ECG Variability During Autonomic Dysreflexia in a Spinal Cord Injury Rat Model”, Military Health System Research Symposium, Kissimmee, FL, August 14-17, 2023.
- Kirby, A. Pancholi, S., Suresh, S., Anderson, Z., Chesler, C., Everett, IV, T.H., Duerstock, B.S. Acclimation Protocol to Minimize Stress in Immobilized Rats During Non-Invasive Multimodal Sensing of the Autonomic Nervous System. *Military Medicine, Warfighters supplement, In press.*
- Kirby, A., Pancholi, S., Anderson, Z., Chesler, C., Everett, IV, T.H., Duerstock, B.S. Time and Frequency Domain Analysis of Physiological Features During Autonomic Dysreflexia after Spinal Cord Injury, *Frontiers in Physiology, under review.*
- Kirby, A.K., Pancholi, S., Suresh, S., Anderson, Z., Chesler, C., Everett, T.H. IV, Duerstock, B.S. “Acclimation Protocol for Spinal Cord Injured Rats to Minimize Stress during Non-Invasive Multimodal Sensing of the Autonomic Nervous System”, Military Health System Research Symposium, Kissimmee, FL, September 12-15, 2022.
- Kirby, A., Pancholi, S., Chesler, C., Anderson, Z., Suresh, S., Sanchez, M., Everett, T.H. IV, Duerstock, B.S. “Identification of Physiological Parameters for Early Detection of Autonomic Dysreflexia after Spinal Cord Injury”, Military Health System Research Symposium, Kissimmee, FL, September 12-15, 2022.